



U.S. DEPARTMENT OF
ENERGY



Ultra-High-Performance Concrete and Advanced Manufacturing Methods for Modular Construction

NEET-1 Annual Meeting
September 29, 2015

Research Team

Y. L. Mo and Mo Li – University of Houston
James G. Hemrick – Oak Ridge National Lab
Maria Guimaraes – Electrical Power Research Institute

Project Monitoring Team

Alison Hahn (Krager) (Project Manager)
Jack Lance (Technical POC)



Self-consolidating Ultra-High Performance Concrete (UHPC)

- A new type of UHPC which features a compressive strength higher than 150 MPa.
- Self-consolidating characteristics
- Desired for SMR modular construction
 - Facilitate rapid construction of steel plate-concrete (SC) beams and walls
 - Thinner and lighter modules
 - Withstands the harsh environments and mechanical loads anticipated during the service life of nuclear power plants

Previous Work and Gaps

- More than two decades of research work on high strength concrete with f_c' more than 100 MPa.
- Direct application in nuclear power plant construction does not yet exist.
- Attaining compressive strengths over 150 MPa without special treatment such as high pressure curing, heat curing and extensive vibration, has remained a challenge
- Lack of standardized processing and quality control methods to produce robust HPC materials in large quantities has limited its application in factory prefabrication.

Experimental Program

- The UHPC material development approach integrates
 - Micromechanics theory
 - Hydration chemistry
 - Rheology tailoring methods
 - Time-dependent computed micro-tomography (Micro-CT)

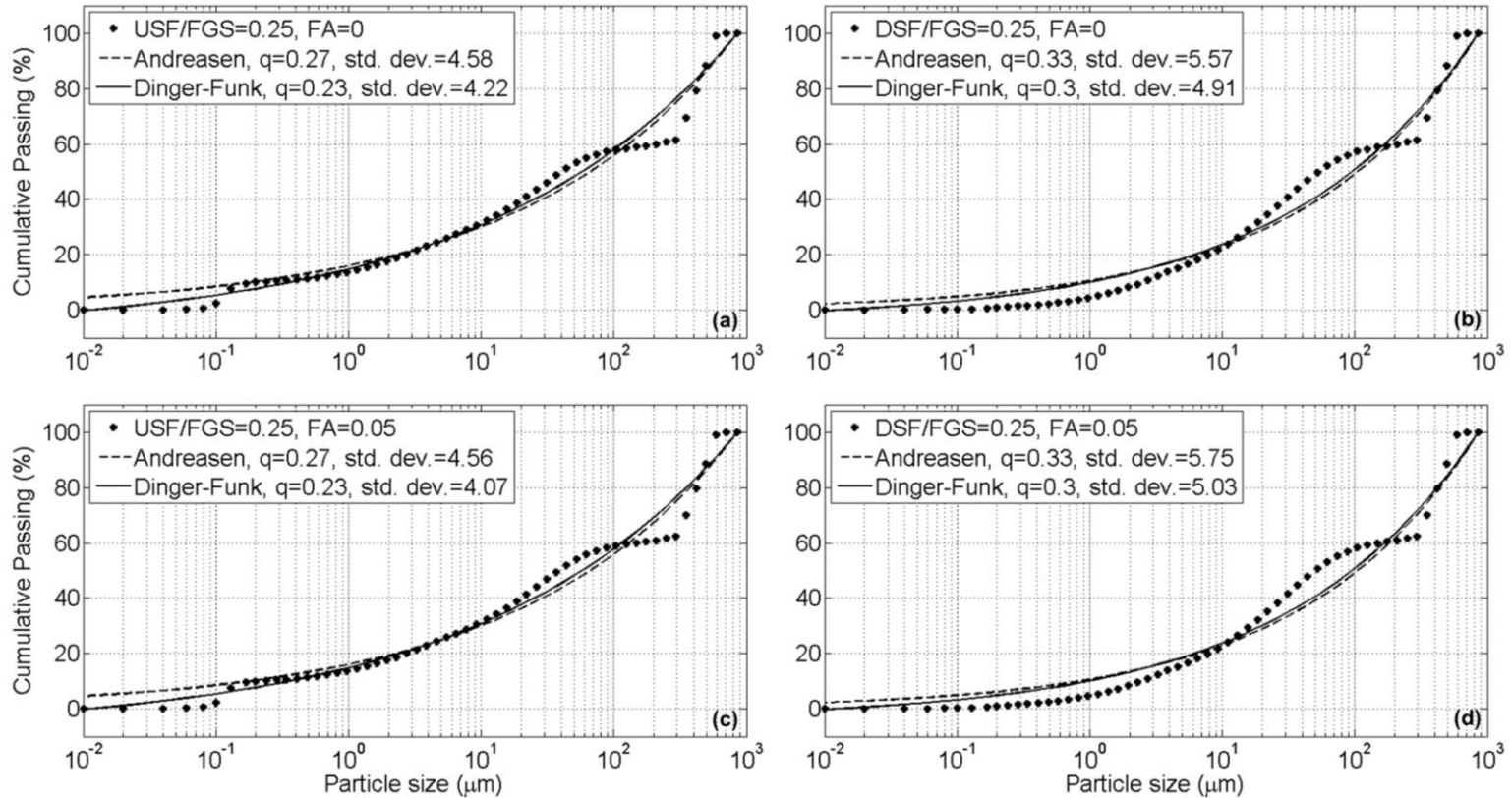
Fundamental Principles for developing UHPC

- **Optimum packing density by selecting ingredients such that all the voids are densely packed.**
- **A low w/b ratio.**
- **Pozzolanic ingredients (e.g. fly ash) with spherical particles to improve workability.**
- **Application of round quartz crystalline silica as high strength aggregates.**
- **Achieving an optimum amount of HRWR.**

Materials

- The UHPC developed in this study contains **cement, silica fume, fly ash, fine sand, aggregates, fine grain silica , high-range water reducer (HRWR) and water.**
- **Cement:** Type I Portland cement (ASTM C150) and Class-H cement
 - Class-H has zero Calcium Aluminate (C_3A) content
 - Class-H has coarser particle size compared to Type I ordinary Portland cement
 - Type I ordinary Portland cement has higher (C_3S) content
- **Silica Fume:** regular densified silica fume (DSF), undensified silica fume (USF) and white silica fume (WSF)
- **Fly ash:** Low calcium Type-F
- **Aggregates:** round quartz crystalline silica that is chemically inert with >99.7% silicon dioxide content.
 - Unground silica passing the sieve size of 850 micron is used as coarse sand
 - Ground silica (GS) passing the sieve size of 212 micron is used as fine sand
- **Fine grain silica (FGS):** Median diameter of the fine ground silica is 1.6 micron, and 96% of the powder has a diameter smaller than 5 micron
- **HRWR (High-range water reducer):** Three different types of Polycarboxylate-based HRWR that are commercially available in the U.S. were investigated, with different amounts of dosage

Experimental Results (Continued)



Particle size distribution of mixtures with 0.25 silica fume, 0.25 FGS, and (a) 5% fly ash, (b) 0% fly ash to cement ratio by weight, compared with PSD models



Developed Ultra-High Performance Concrete

- 150 MPa (22 ksi) compressive strength
- Self-consolidating property
- High durability
- No special (curing) treatment required

Optimum mixture proportions:

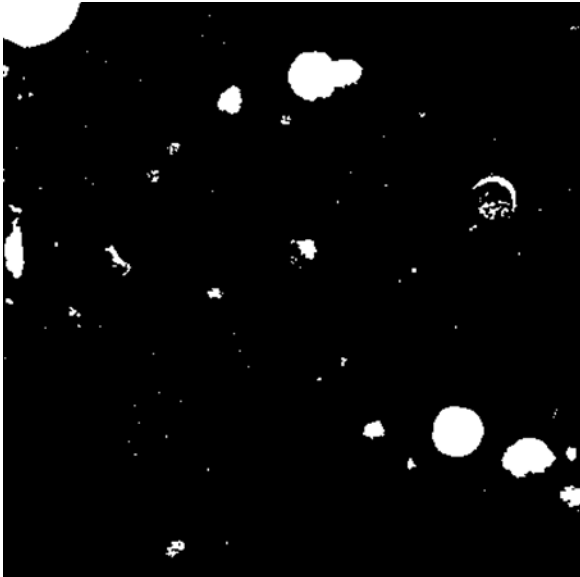
Ingredient	Proportion
Cement	1
Silica Fume (Undensified)	0.200
Fly Ash	0.050
Silica Powder	0.200
w/b	0.210
Superplasticizer (HRWR)	0.060
Sand 1 (0.212mm)	0.28
Sand 2 (0.85mm)	1.12

Test Results	
Spread Value (cm)	26
f'_c (ksi)	23.24

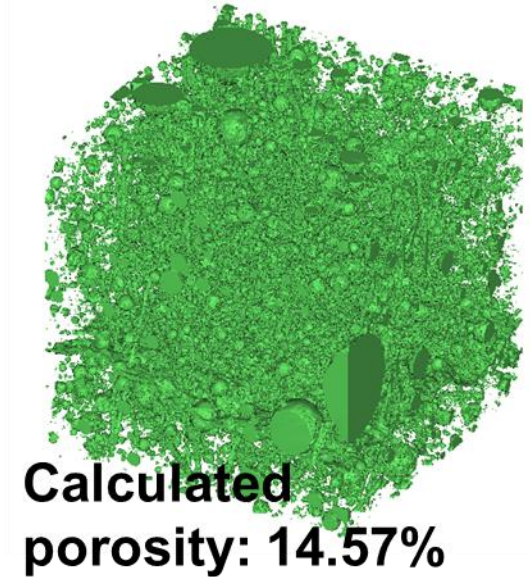
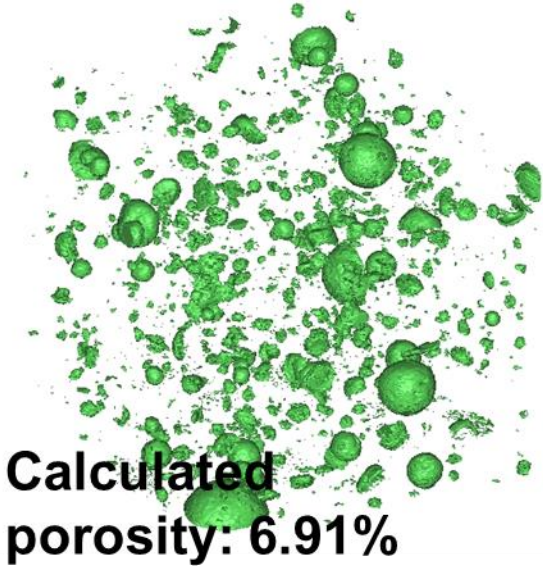
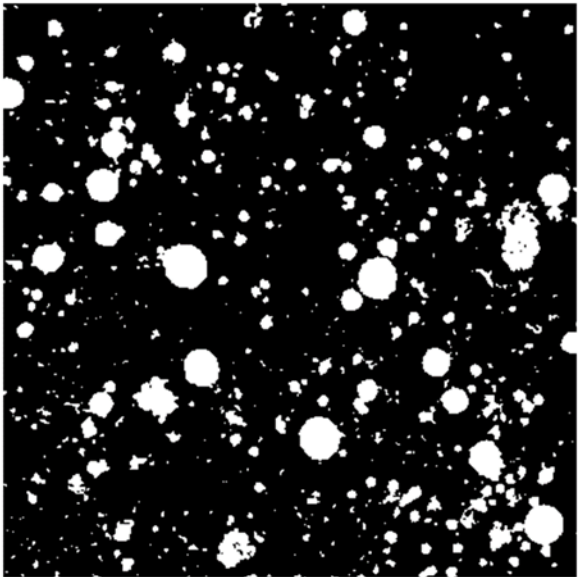
UHPC Microstructure Characterization



UHPC



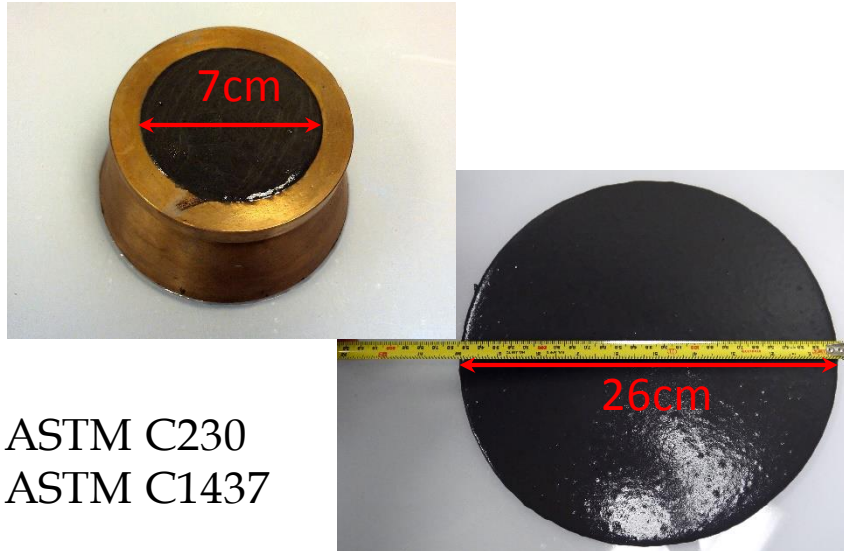
Conventional Mortar



Self-Consolidating Characterization



- Small scale, 5 Qt. capacity



ASTM C230
ASTM C1437

- Large scale, 11 ft³ capacity



ASTM C143, ASTM C1611

Self-consolidating UHPC



V-funnel test



Passing ability test
(J-ring)



During casting of Steel-plate UHPC beam,
good flowability demonstrated without vibration

Self-consolidating UHPC (Continued)



- UHPC self-consolidating properties ($f_c' = 22.34$ ksi)

Test	UHPC	EFNARC
Slump flow by Abram's cone	77 cm	65-85 cm
$T_{50\text{cm}}$ slump flow	4 sec	2-5 sec
J-ring, height difference	0-2 mm	0-10 mm
V-funnel	10 sec	6-12 sec
V-funnel increase time at $T_{5\text{min}}$	7 sec	3 sec
J-ring, spread difference	0 cm	N/A
Visual stability index (ASTM C1611)	0	N/A
Air content	4.8%	N/A

Note: EFNARC: The European Guidelines for Self-Compacting Concrete

Structural Behavior of S-UHPC Modules

- Integrity between two distinct materials (UHPC and steel-plate) is essential.
- Integrity through effective shear transfer mechanism
- Shear transfer mechanisms:
 - a) Tie bars (Cross Ties)
 - b) Shear studs
 - c) J-hook
 - d) Profiled and surfaced preparation

Design Codes and Guidelines

for minimum shear reinforcement ratio

- No technical document available for design of cross ties.
- Designers use four codes commonly used in design of SC structures: (a) ACI 349 Code (2013), (b) Model Code, (c) Design guide by Steel Construction Institute (Narayan et al. 1994), (d) JAEG (2005)
- Design guidelines (c) and (d) do not specify the minimum shear reinforcement ratio.
- ACI 349 Code adopts ACI 318 Code which is for RC members
- Minimum shear reinforcement ratio for reinforced concrete (RC) specified by ACI 318 Code $\rho_{t,ACI}$ is:

$$\rho_{t,ACI} = 0.75 \frac{\sqrt{f'_c}}{f_{yt}} \geq 50 \frac{1}{f_{yt}}$$

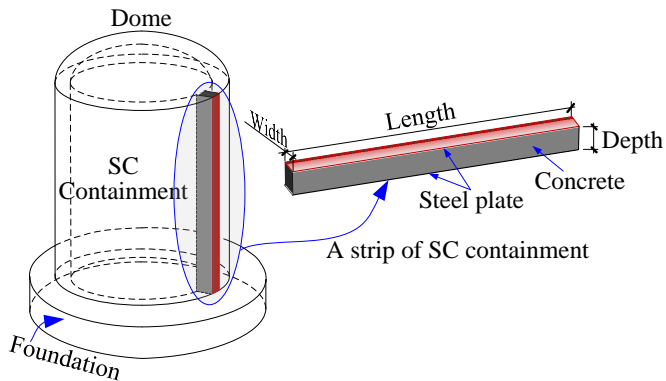
- The *fib* Model Code 2010 requires the minimum shear reinforcement ratio $\rho_{t,fib}$ for RC members, as specified by Eq. 8 (fib 2010; Sigrist et al. 2013).

$$\rho_{t,fib} = 0.08 \frac{\sqrt{f_{ck}}}{f_{yk}} \quad (f_{ck} \text{ and } f_{yk} \text{ in MPa})$$

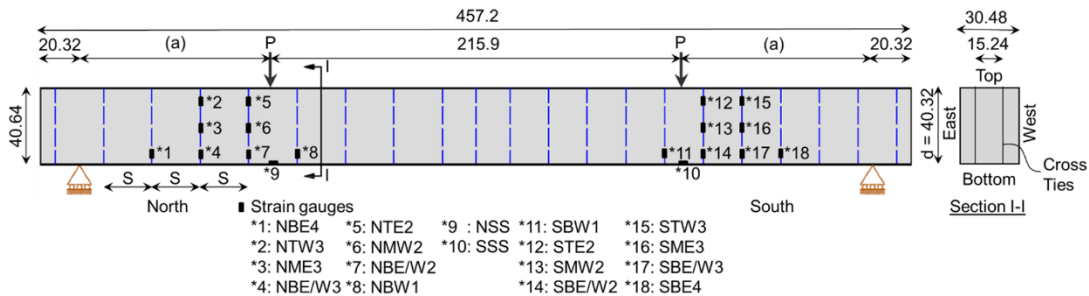
Experimental Program

(S-UHPC Beams)

- A strip of nuclear containment is taken out as the study specimen and it is scaled down by a factor of 4/9.



SC Nuclear Containment



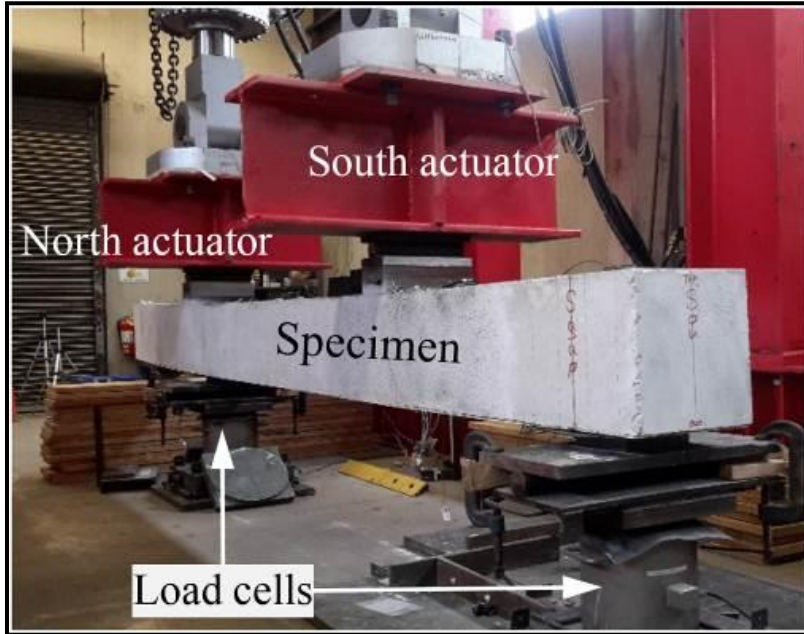
Elevation and strain gauge arrangement of S-UHPC beam

Two SC beams (S-UHPC1 and S-UHPC2) were tested.

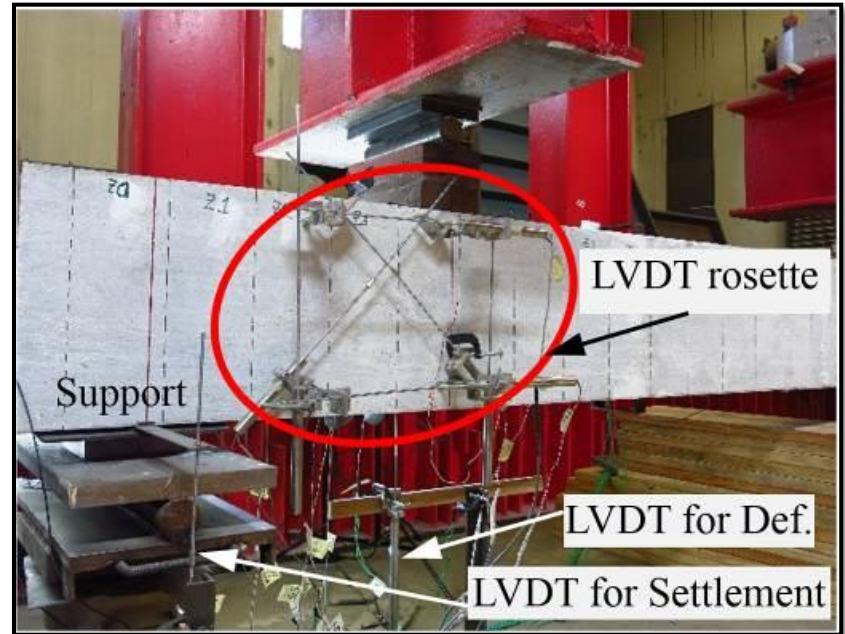
The length, width, and depth of each SC beam are 4572 mm (15.0 ft.), 304 mm (12.0 in.), and 406 mm (16.0 in.), respectively.

The only test parameter was the Cross ties ratio ($\rho_{t,test}$).

Test Setup

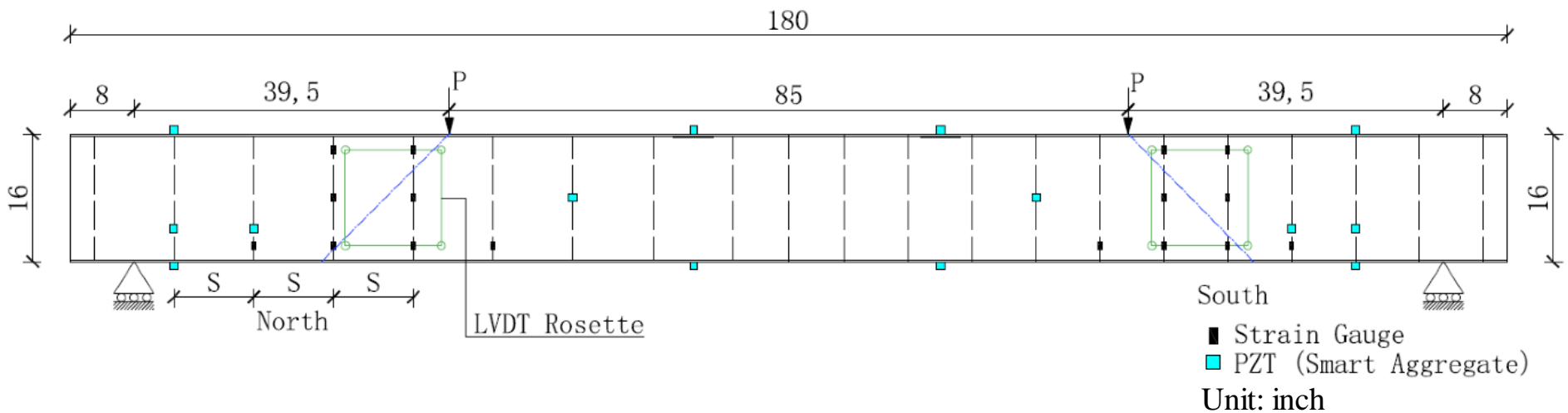


Loading arrangement



Setup of LVDT

Instrumentation



Typical SC beam and arrangement of strain gauges and SAs

Experimental Matrix

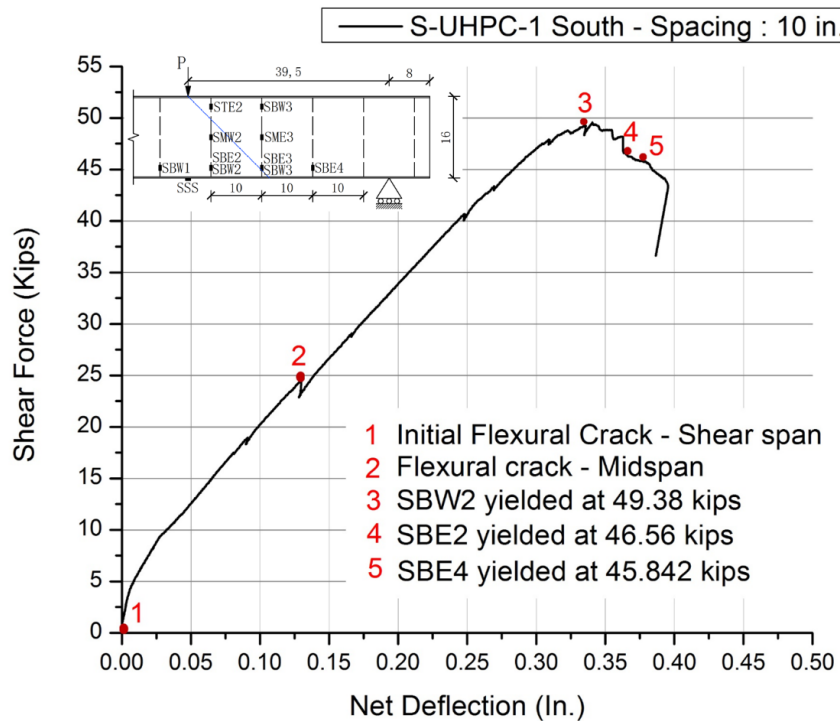
Specimen	$s_{tie}^{\#}$ (cm)	$f_c^{'*}$ (MPa)	$\rho_{t,ACI}$ (%)	$\rho_{t,test}$ (%)	$\rho_{t,test}/\rho_{t,ACI}$	$F_{peak.}^{**}$ (kN)	Ductility δ^{\dagger}	Failure Mode
S-UHPC-1 South	25.4	154.0	0.170	0.184	1.08	220.5	1.003	Ductile
S-UHPC-2 South	17.1	153.89	0.170	0.277	1.63	345.6	2.650	Ductile
S-UHPC-2 North	14.6	153.89	0.170	0.323	1.90	381.7	4.010 \yen	Ductile

Experimental matrix, strength, and failure mode

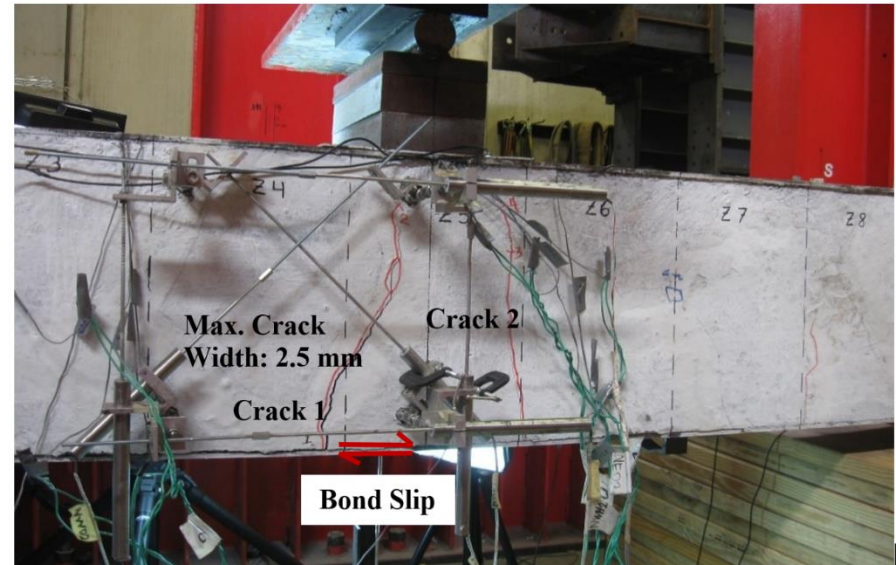


Casting of S-UHPC beam

Results: S-UHPC-1 South

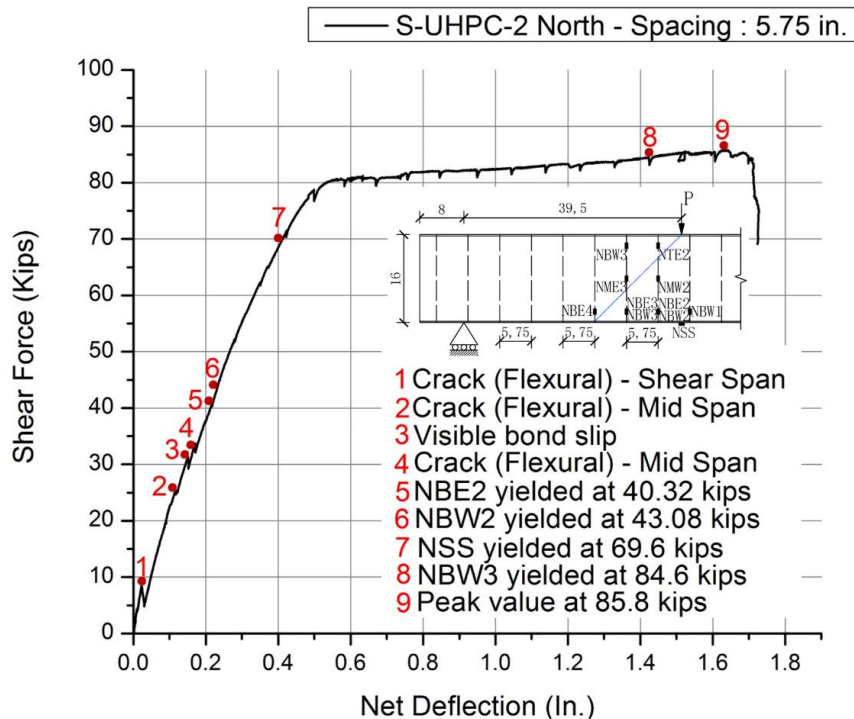


Shear-force deflection curve

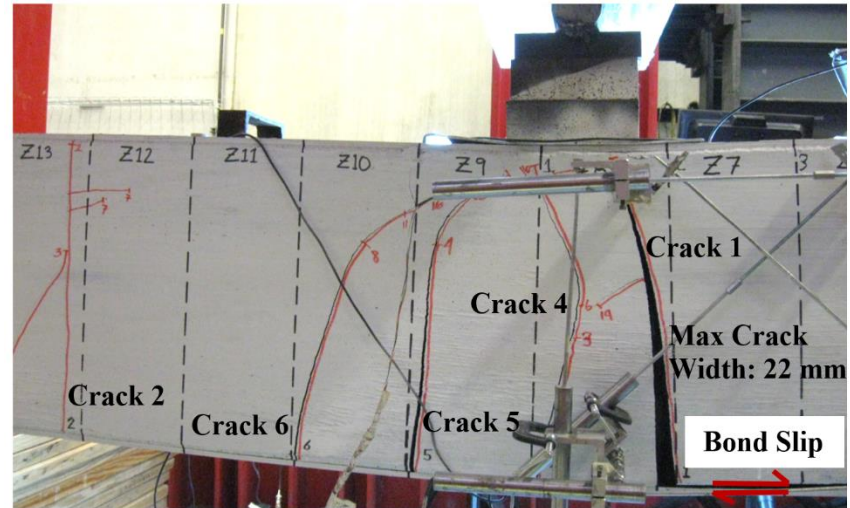


Crack Pattern at Failure Mode

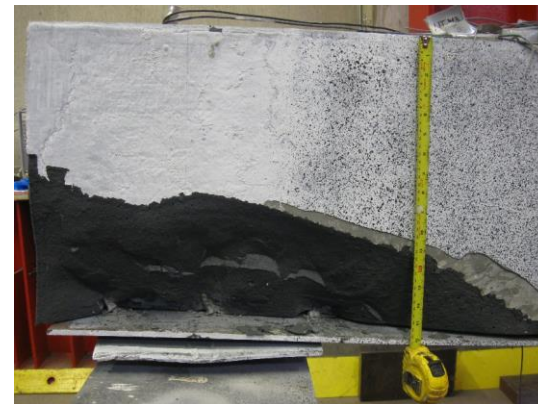
S-UHPC-2 (North)



Shear-force deflection curve

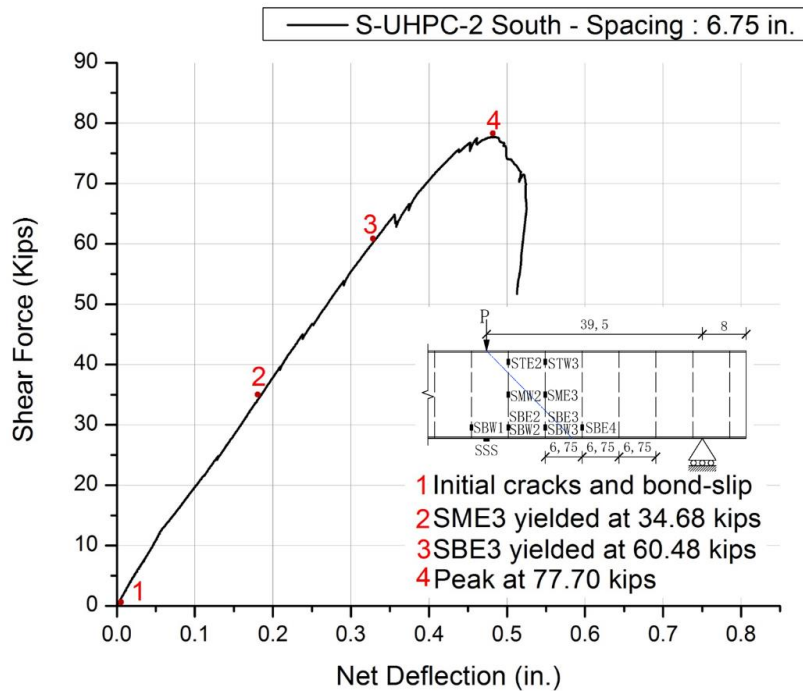


Crack Pattern at Failure Mode

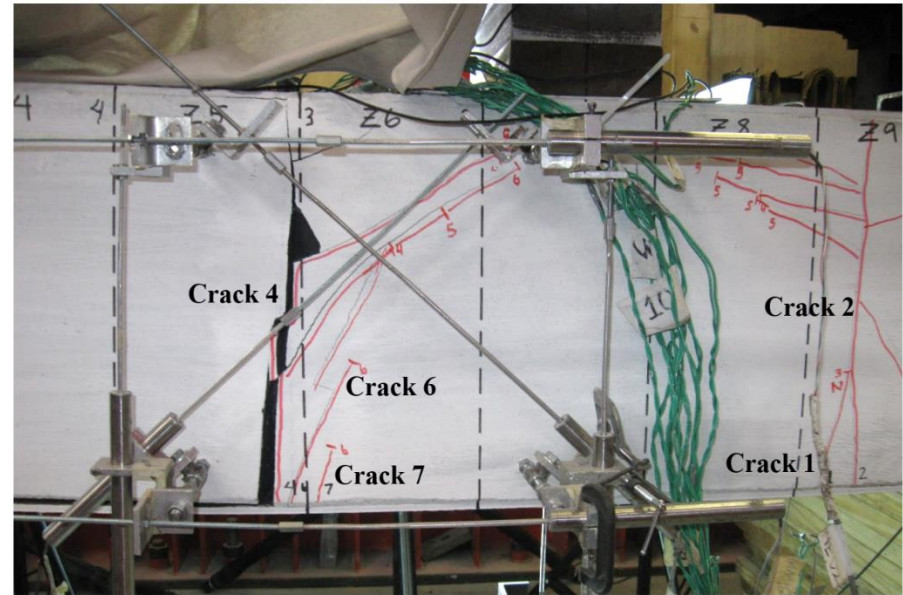


Spalling of concrete

S-UHPC-2 (South)



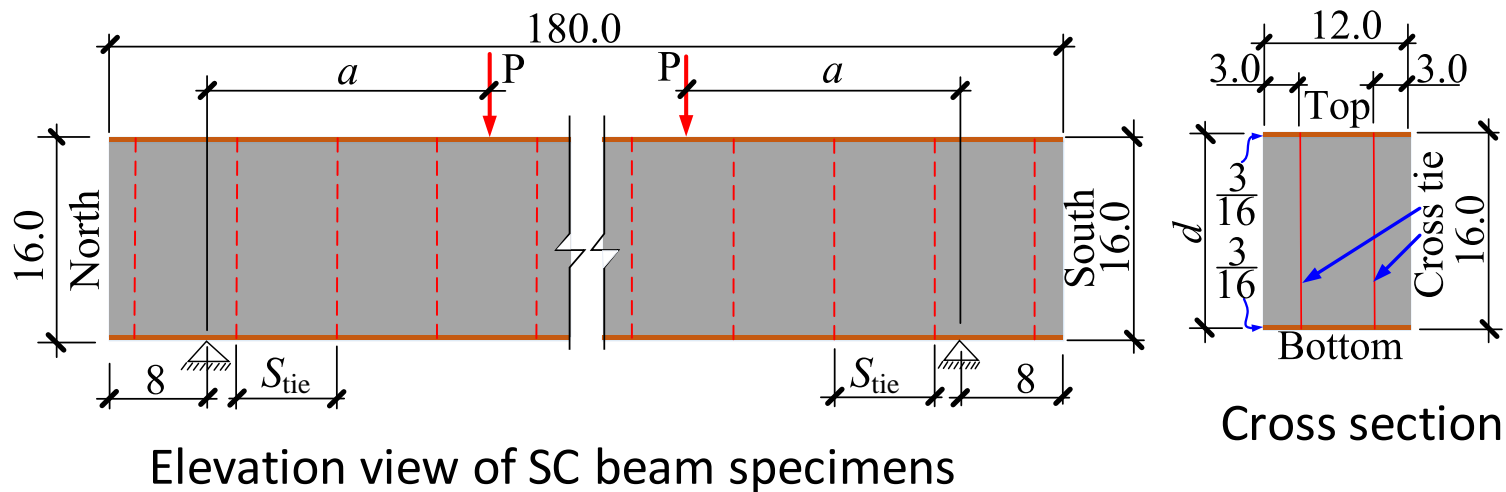
Shear-force deflection curve



Crack Pattern at Failure Mode

(SC Beams) as reference of S-UHPC beams

- To evaluate the effect of concrete strength on the structural performance of Steel plate Concrete (SC) beams with conventional concrete, six SC beams were tested
- Same size as S-UHPC beams



Dimensions of SC beam specimens (unit: inch)

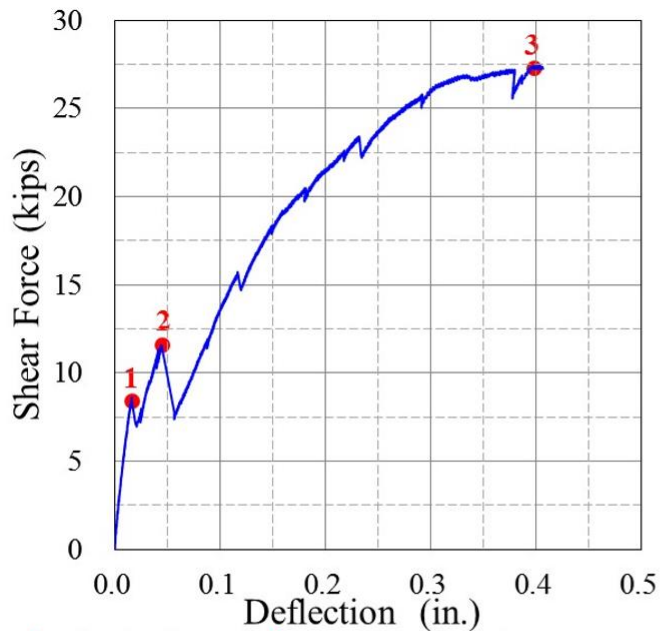
Experimental Matrix

Normal strength concrete

Specimen	a/d	S_{tie} (in.)	f'_c (ksi)	$\rho_{t,ACI}$ (%)	$\rho_{t,test}$ (%)	$\rho_{t,test}/\rho_{t,ACI}$	$F_{ult.}$ (kips)	Ductility δ	Failure Mode
SC1 north	2.5	8.00	8.13	0.111	0.102	0.92	27.4	—	Brittle
SC1 south	2.5	8.00	8.13	0.111	0.102	0.92	26.1	—	Brittle
SC2 south	2.5	7.00	5.80	0.094	0.117	1.25	26.9	0.730	Brittle
SC3 north	2.5	6.00	5.82	0.094	0.137	1.45	31.7	1.17	Ductile
SC3 south	2.5	6.00	5.82	0.094	0.137	1.45	34.9	1.79	Ductile
SC4 north	2.5	5.00	7.37	0.106	0.164	1.54	42.7	1.58	Ductile
SC4 south	2.5	4.00	7.37	0.106	0.205	1.93	53.0	1.65	Ductile
SC5 south	1.5	6.00	8.00	0.110	0.137	1.25	55.9	1.43	Ductile
SC5 north	1.5	5.00	8.00	0.110	0.164	1.49	64.7	1.48	Ductile
SC6	5.2	6.00	8.00	0.110	0.137	1.25	29.3	1.99	Ductile

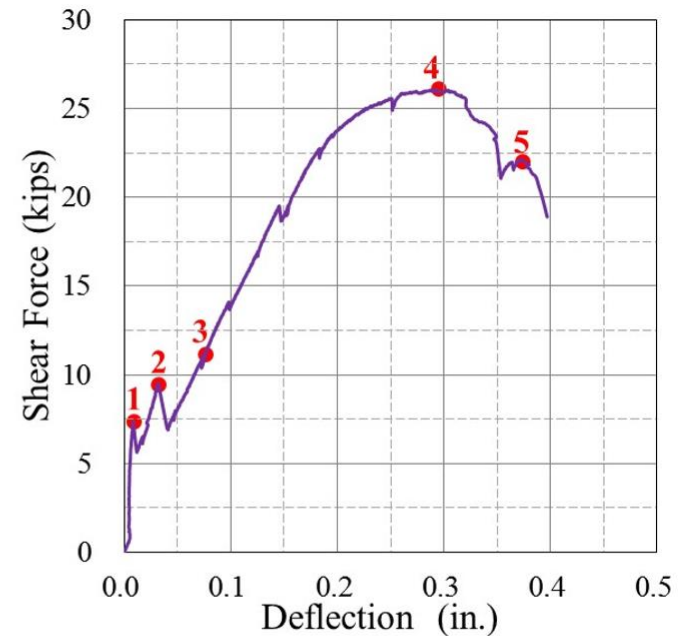
Test Results

Specimen SC1



- 1:** Crack (flexural) **2:** Crack in north shear span
3: Peak point

(a) North side

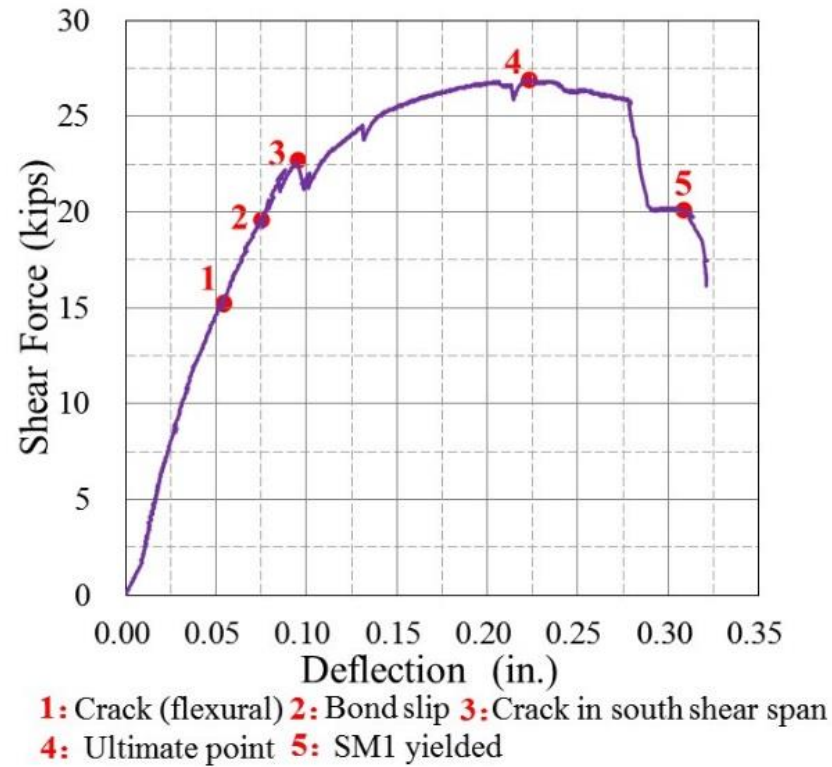


- 1:** Crack flexural **2:** Crack in the south shear span
3: Crack in the south shear span **4:** Ultimate point
5: Lost capacity

(b) South side

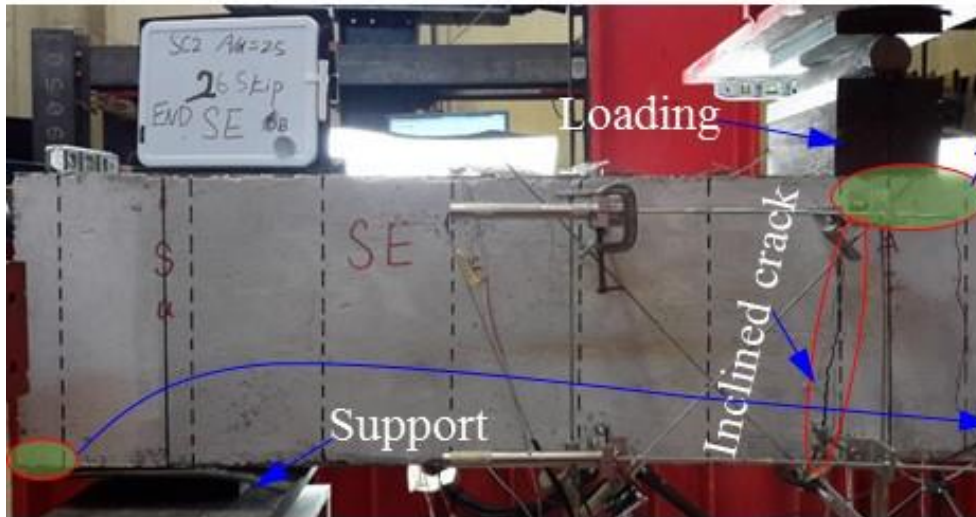
Figure Shear force-deflection curves of SC1

Specimen SC2 South



Shear force-deflection curve of SC2 South

Specimen SC2 South (Continued)



(a) Crack pattern



(b) Crack close top steel plate

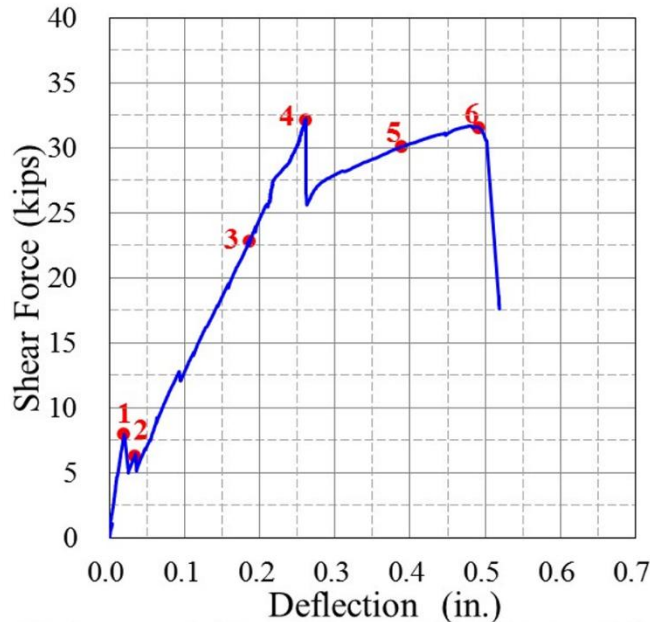


(c) Bond slip near support

Crack pattern and debonding of SC2 south after test

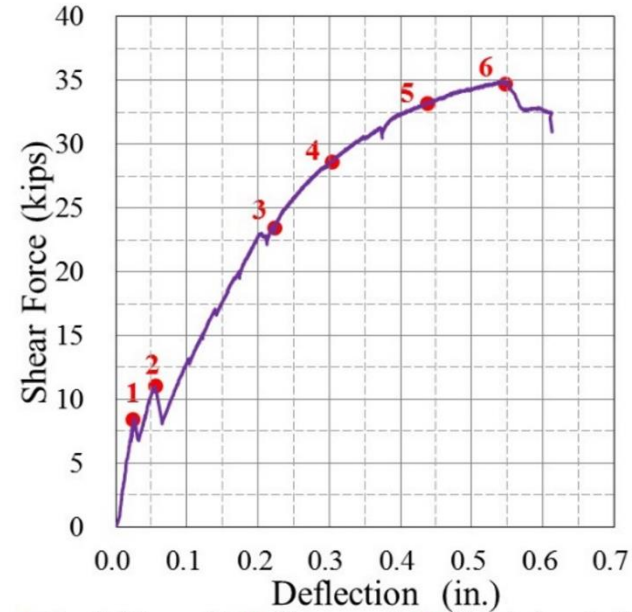
Specimen SC3

(Cross tie 45% more than that specified in ACI code)



1: Shear Crack 2: Crack(flexural) 3: Visible bond slip
4: Critical shear crack 5: NT1 yielded 6: Ultimate point

(a) SC3 north

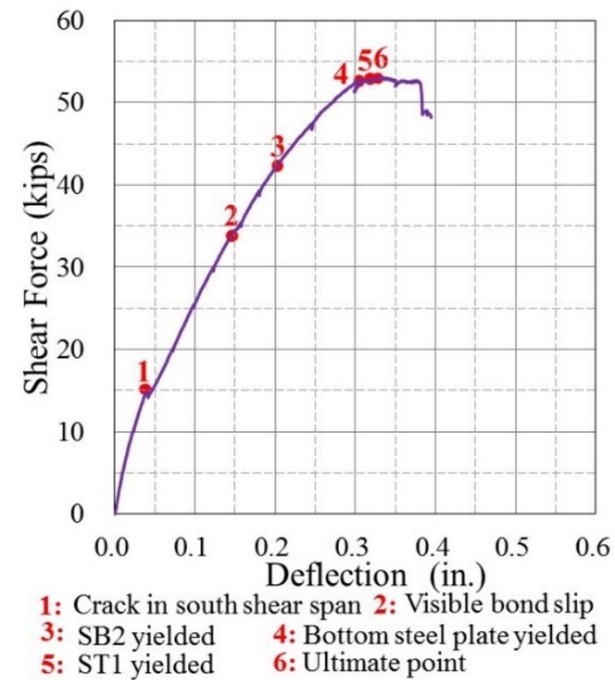
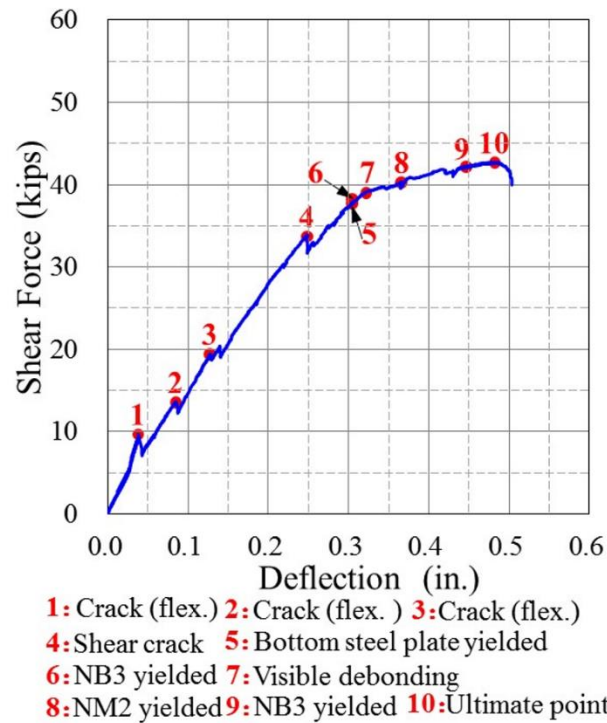


1: Crack (flexural) 2: Shear crack 3: Visible bond slip
4: SB1 yielded 5: SM1 yielded 6: Ultimate point

(b) SC3 south

Shear force-deflection curves of SC3

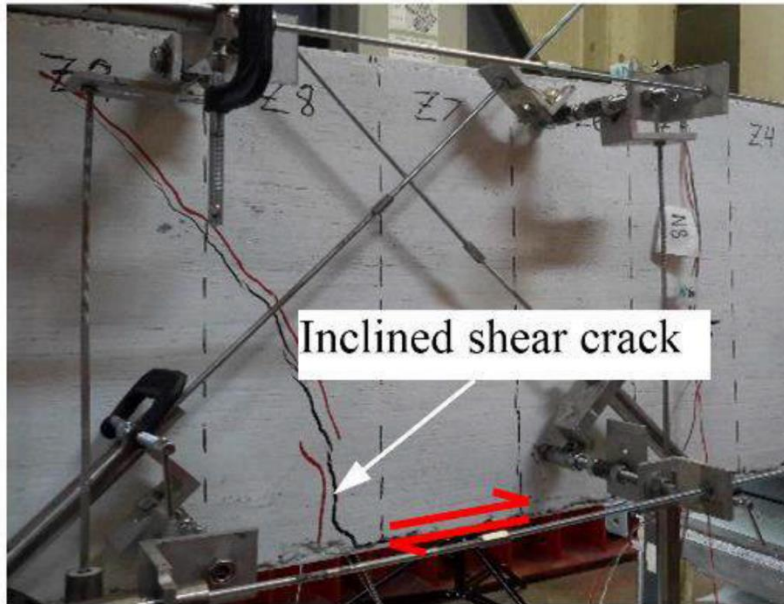
Specimen SC4



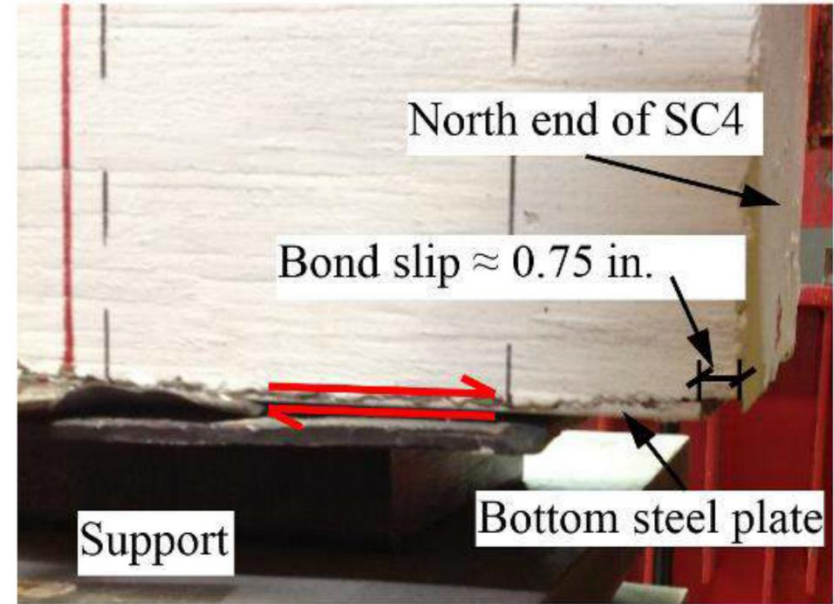
(a) SC4 north of cross ties spacing at 5 in. (b) SC4 south of cross ties spacing at 4 in.

Shear force-deflection curves of SC4

Specimen SC4 (Continued)



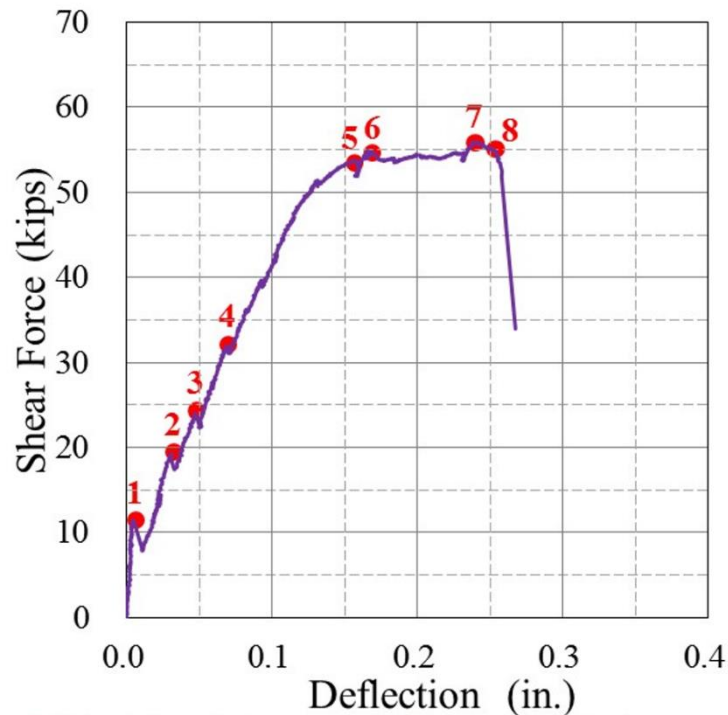
(a) At the peak load stage



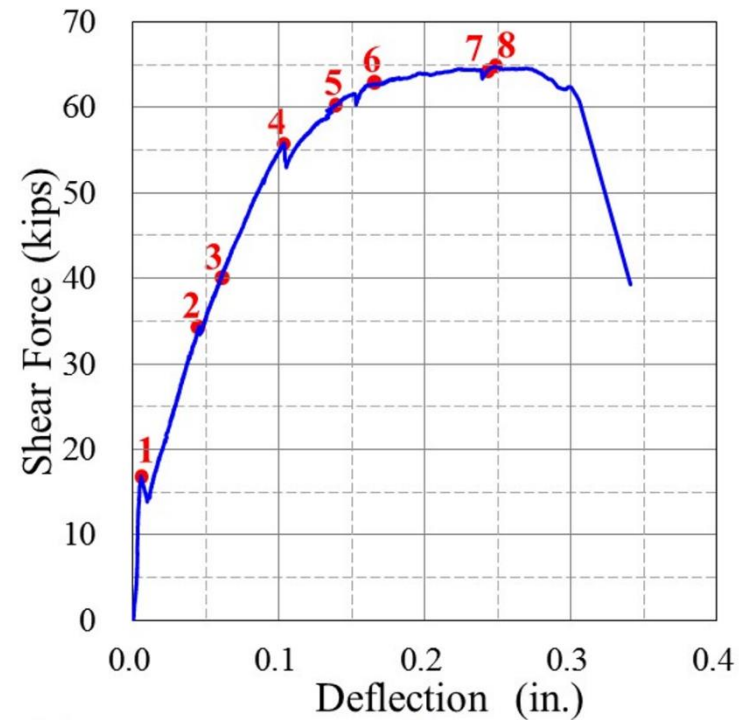
(b) At the post peak stage

Critical shear crack and bond slip of SC4 north

Specimen SC5



- 1:** Crack(south shear span) **2:** Crack (south shear span)
3: Crack(flex.) **4:** Crack (flex.) **5:** Visible bond slip
6: SB2 yielded **7:** Ultimate point **8:** SM1 yielded

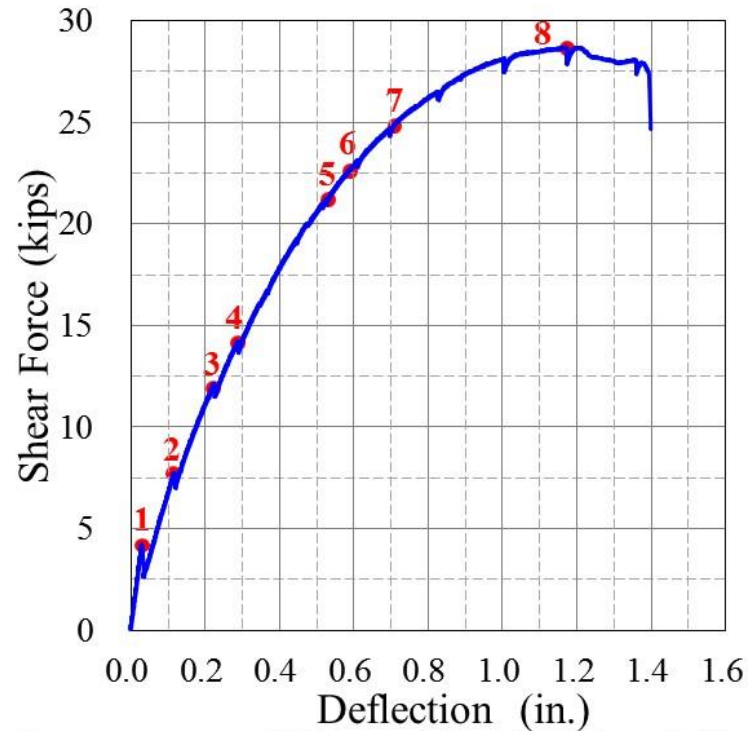


- 1:** Crack (north shear span) **2:** Crack (north shear span)
3: Crack (flex.) **4:** Crack extended **5:** Visible bond slip
6: NB2 yielded **7:** NM1 yielded **8:** Ultimate point

(a) SC5 south of cross ties spacing at 6 in. (b) SC5 north of cross ties spacing at 5 in.

Shear force-deflection curves of SC5

Specimen SC6

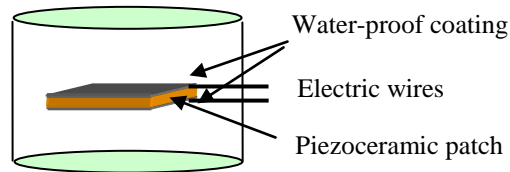


- 1:** 1st crack (flex.) **2:** 2nd crack (flex.) **3:** 3rd crack (flex.)
4: 4th crack (flex.) **5:** Bottom steel plate yielded
6: ST2 yielded **7:** Visible bond slip **8:** Ultimate point

Shear force-deflection curve of SC6

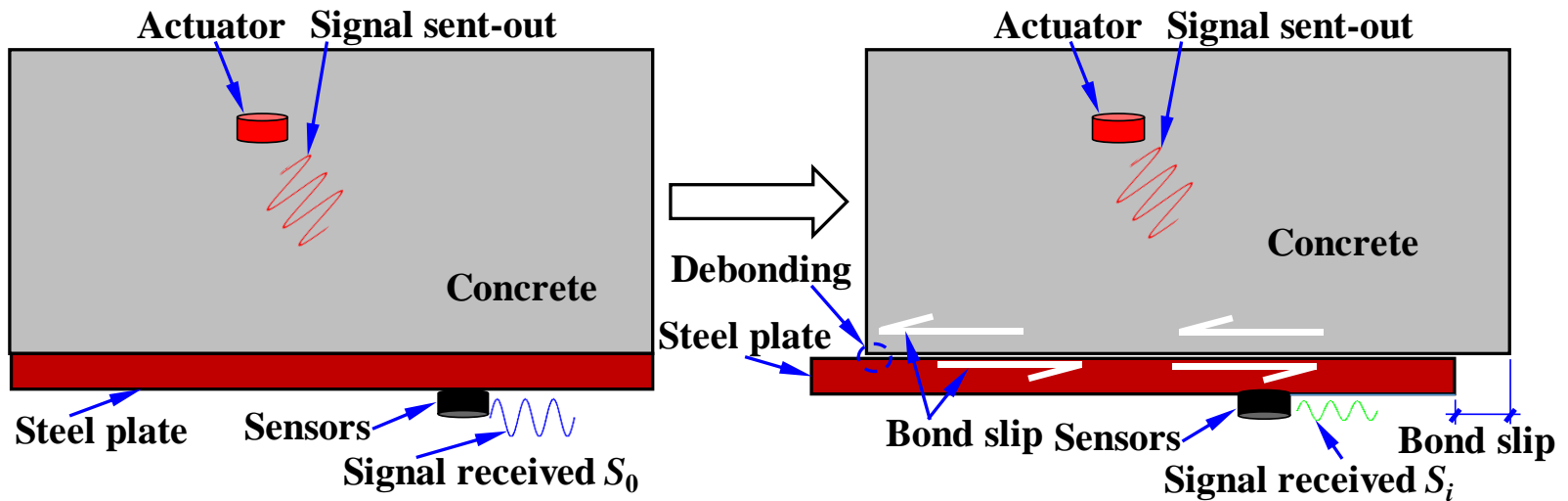
Bond slip detection between steel plate and concrete using smart aggregates

- Inaccessibility and invisibility of the interface.



- Piezoceramic-based Smart Aggregates (SAs)
 - Proved applicable to health monitoring and damage detection.

Detection principles



Developed smart aggregate based active sensing approach to detect bond slip between steel plate and concrete

Test details

Two selected SC beams

Specimen	a/d	$S_{tie}^{\#}$ (in.)	f'_c [*] (ksi)	$F_{ult.}$ ^{**} (kips)	$\rho_{t,ACI}$ (%)	$\rho_{t,test}$ (%)	$\rho_{t,test}/\rho_{t,ACI}$
SC1 North	2.50	8.00	8.13	27.4	0.111	0.102	0.92
SC1 South	2.50	8.00	8.13	26.1	0.111	0.102	0.92
SC4 North	2.50	5.00	7.37	42.7	0.106	0.164	1.54
SC4 South	2.50	4.00	7.37	53.0	0.106	0.205	1.93

S_{tie} = the spacing of cross ties.
*** f'_c = the concrete compression strength from concrete cylinders (152.4 mm × 304.8 mm).**
**** $F_{ult.}$ = ultimate shear capacity**

Installation and location of SAs

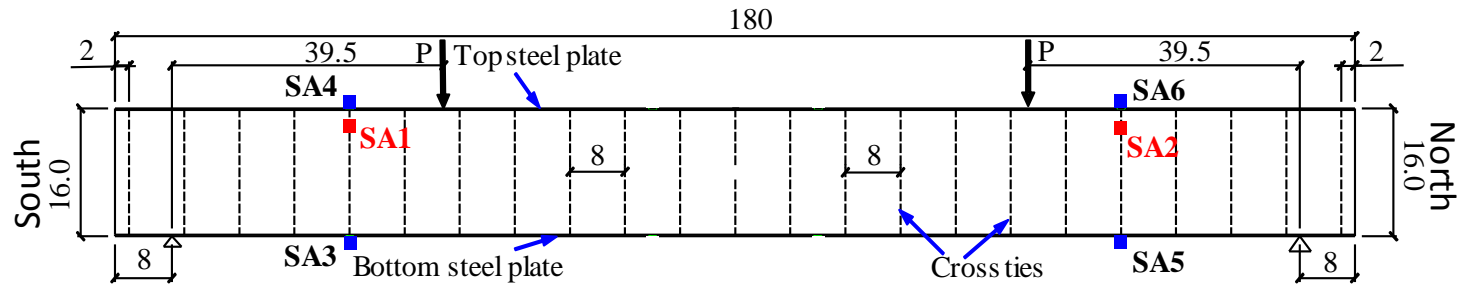


Figure Arrangement of SAs in SC1 (unit: inch)

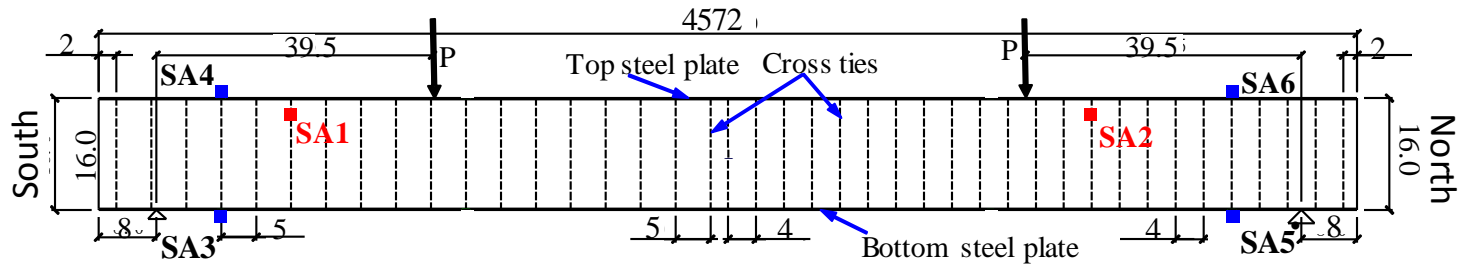
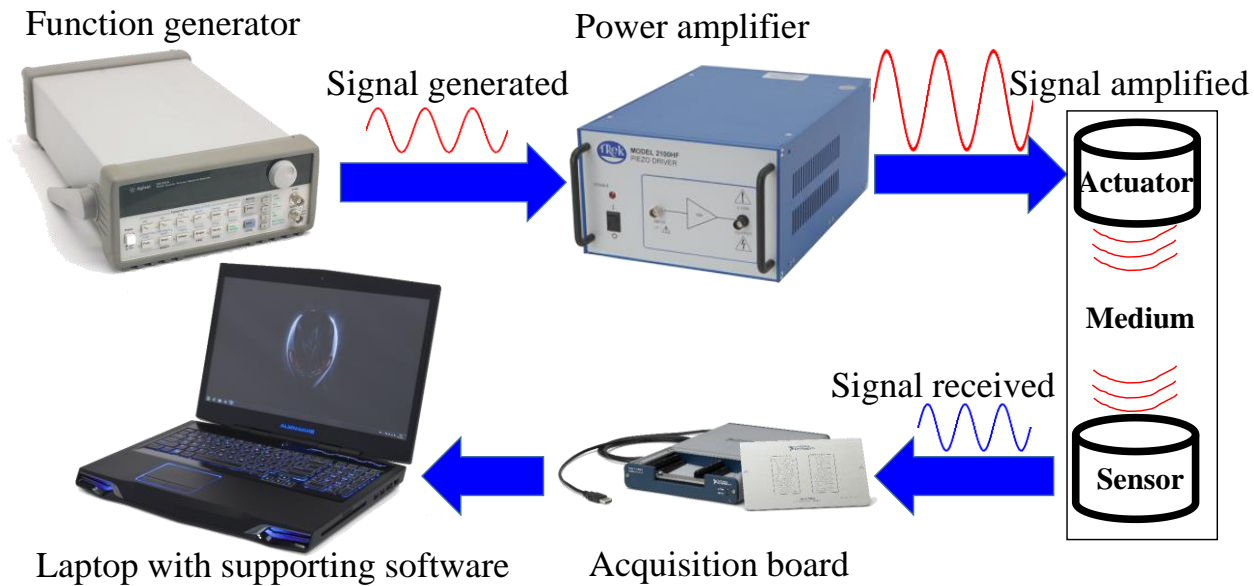


Figure Arrangement of SAs in SC4 (unit: inch)

Apparatus

- Function Generator
- Power Amplifier
- Data Acquisition board



Apparatus Setup

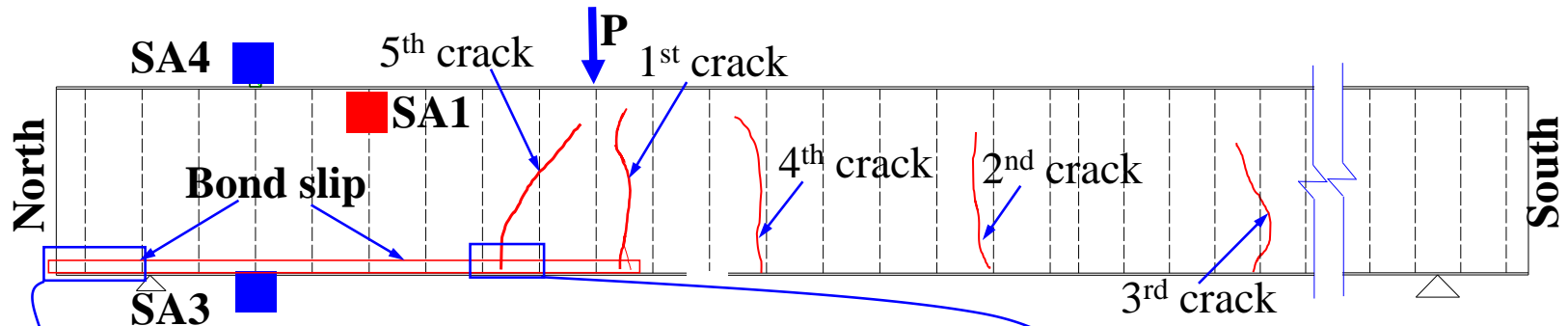
SC1 North

SC1 South

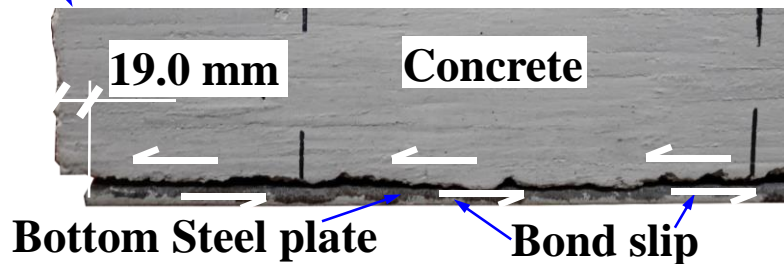


Function generator DAQ board Power amplifier Laptop

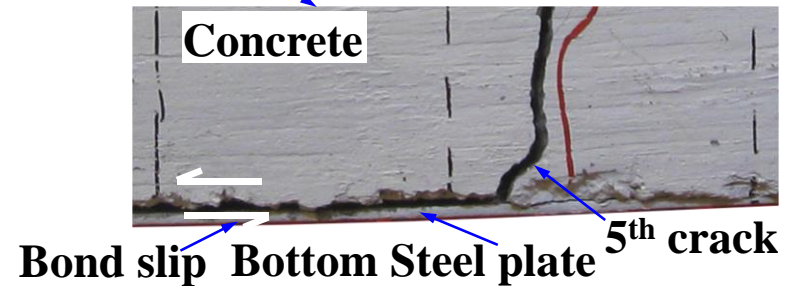
Sample Test Result (SC4 North)



(a) Location of bond slip and crack



(c) Bond slip at north end (side)



(b) Crack and bond slip

Bond slip and crack patterns in SC2 north after test

SC4 North

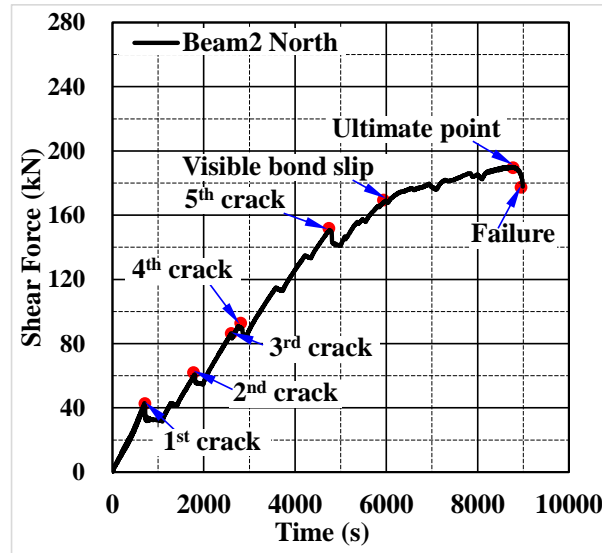


Fig. 32. Shear force-time curves of SC4 north

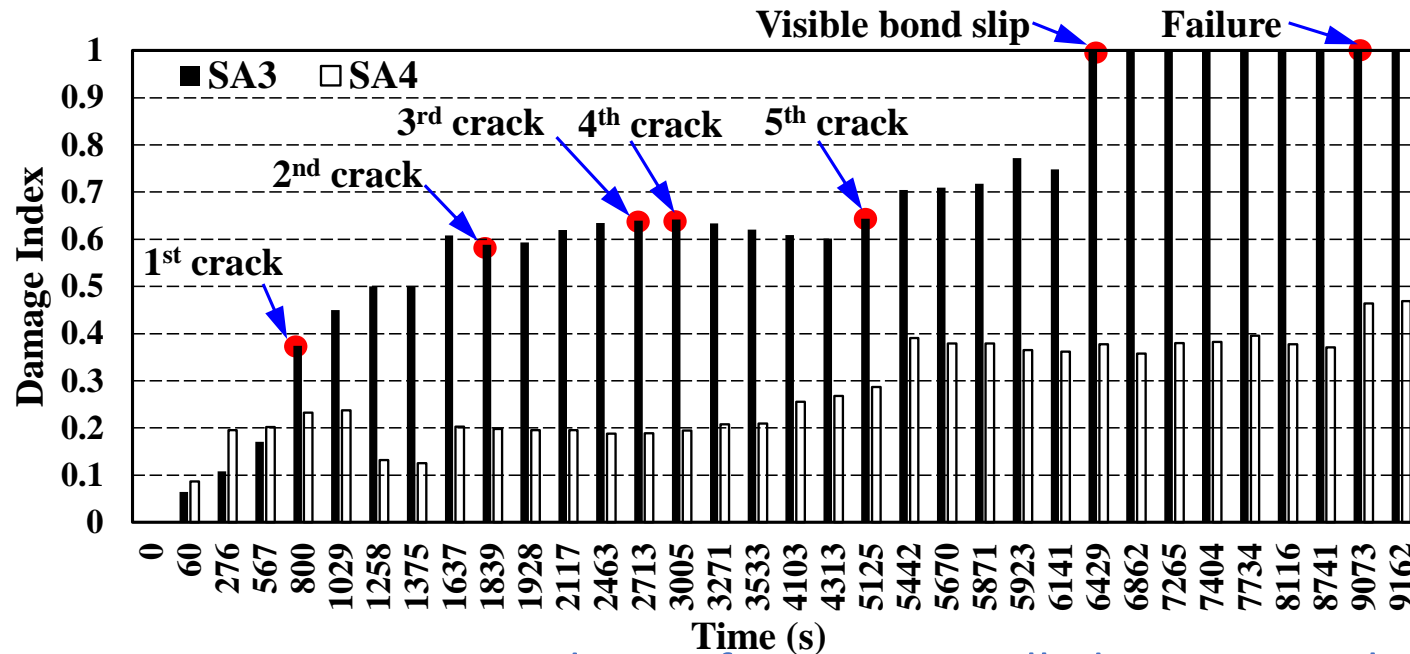
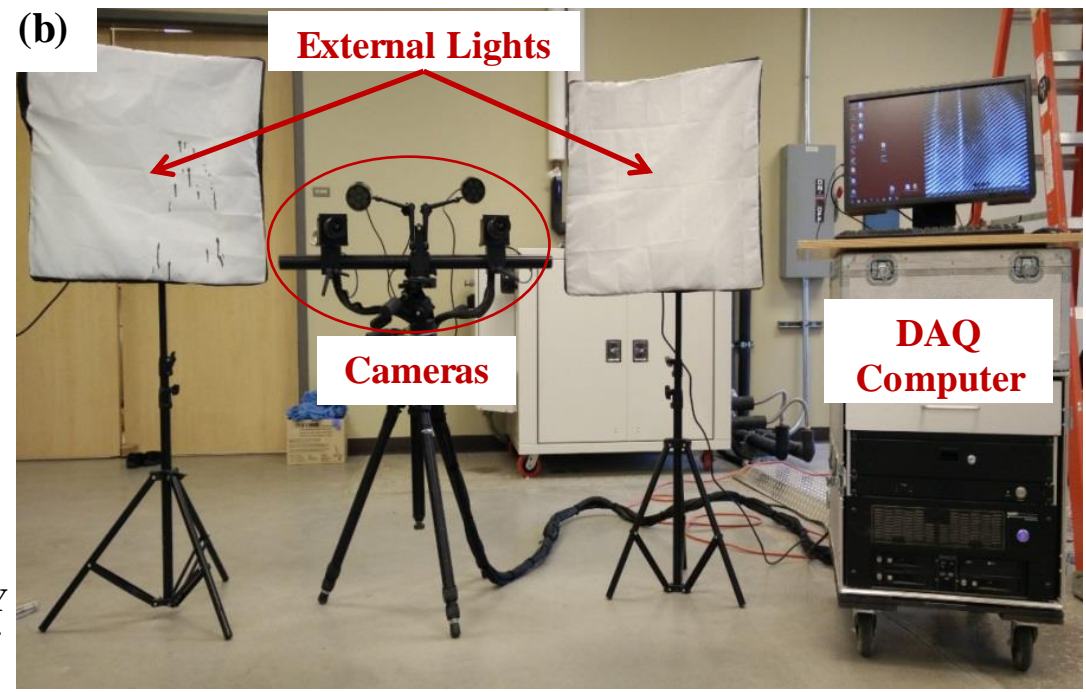
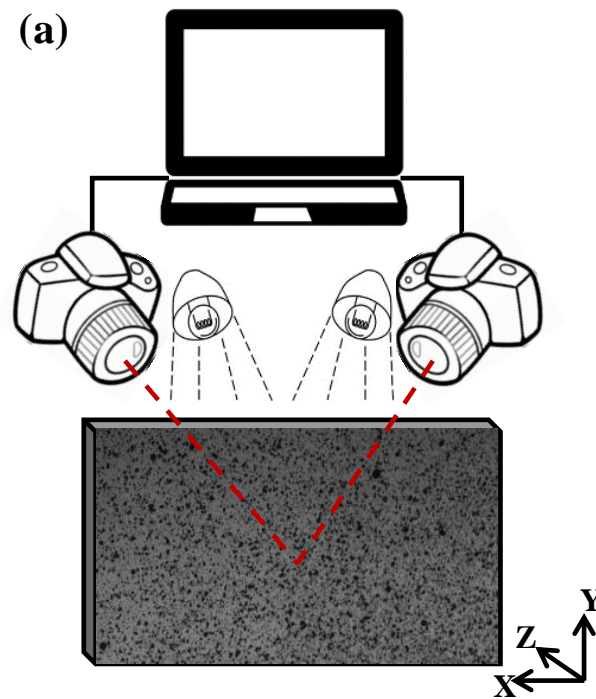


Figure Damage indexes of sensors installed on SC4 north

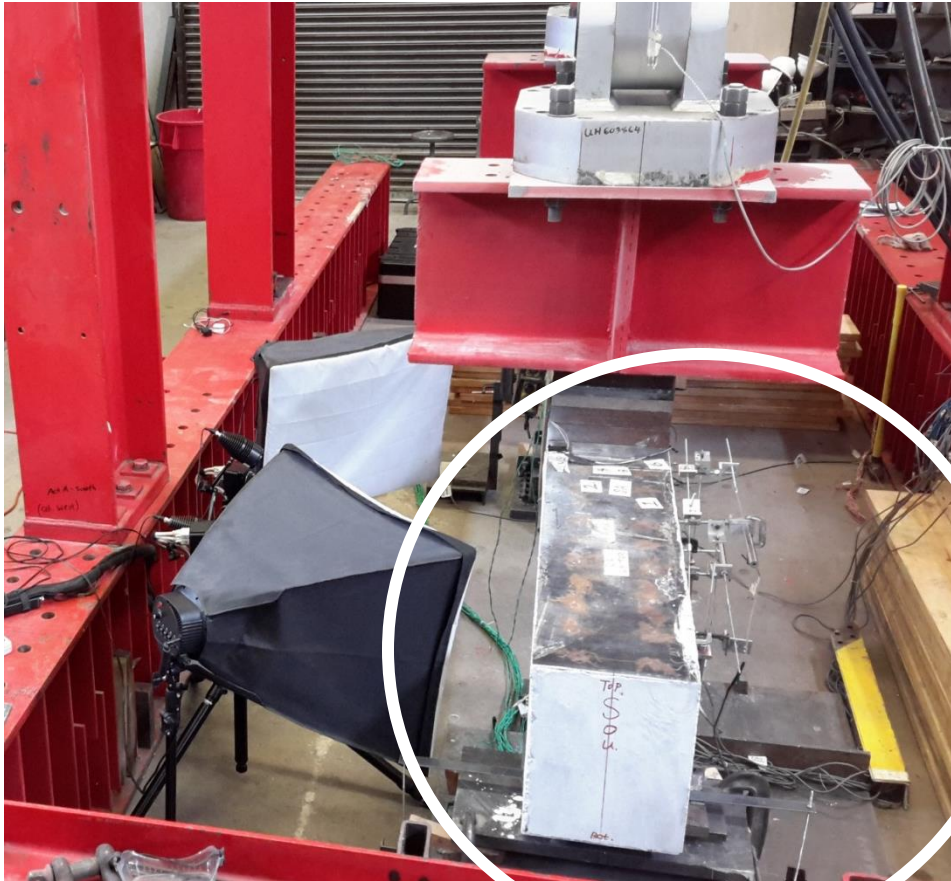
Digital Image Correlation-Based Debonding Detection

Instrumentation



DIC system setup, (a) Schematic illustration, (b) Pictorial illustration

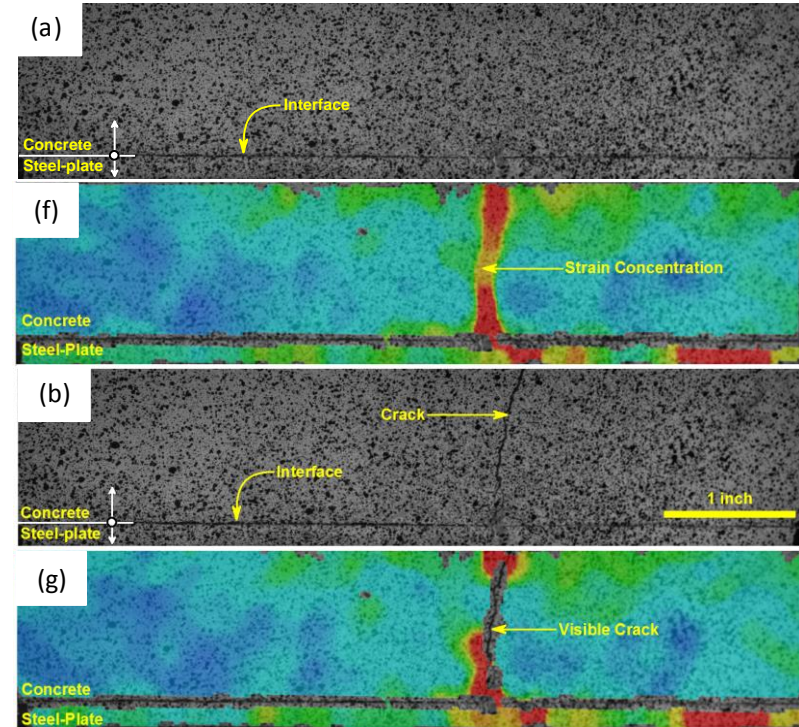
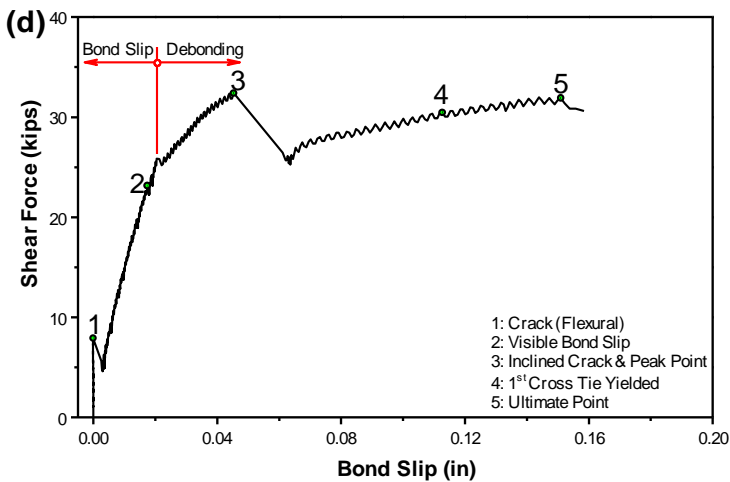
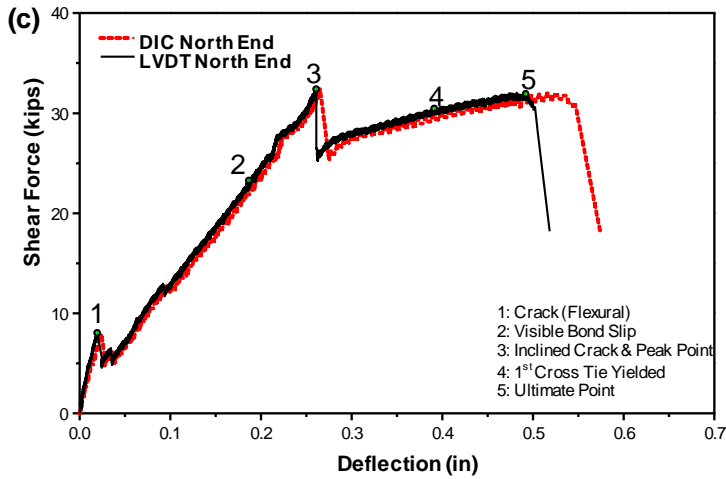
Test Setup



The results from DIC is used to compute:

1. Beam deflection
2. Strain contour map
3. Point-to-point average strain
4. Crack opening
5. Steel concrete debonding
6. Final localization with $\pm 5 \mu\text{m}$ accuracy

Discussion on Debonding

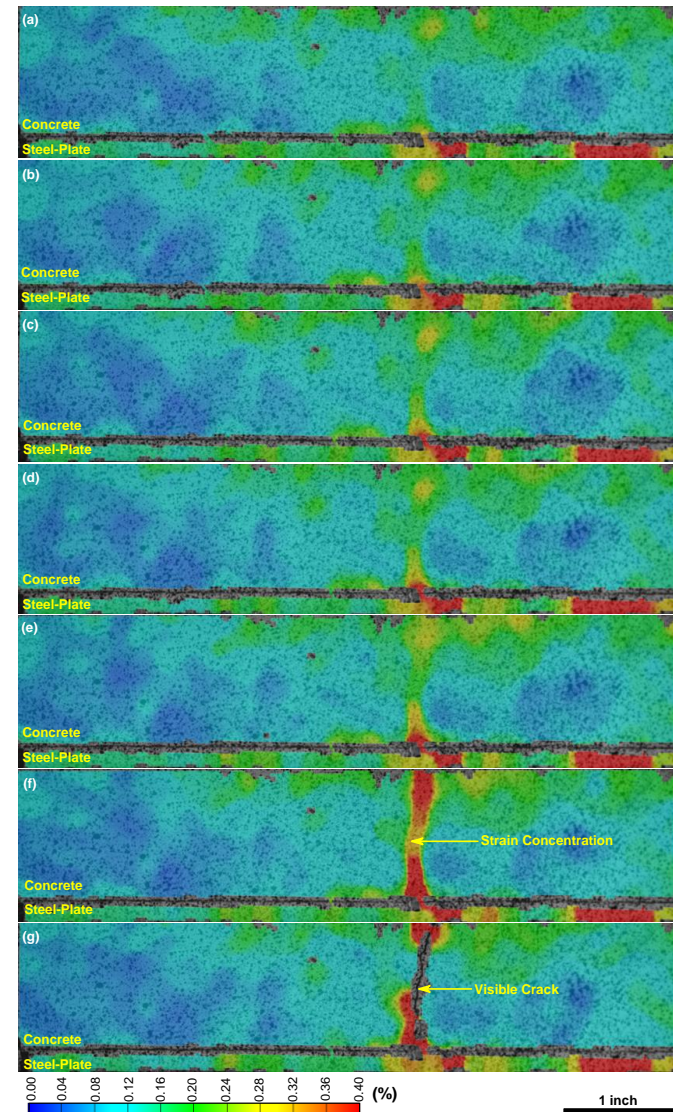


High-resolution images (a) and DIC image (f) of SC3 at north-end corresponding to point 3 in Figs. (c) and (d).
(b) and (g) right after point 3 in Figs. (c) and (d).

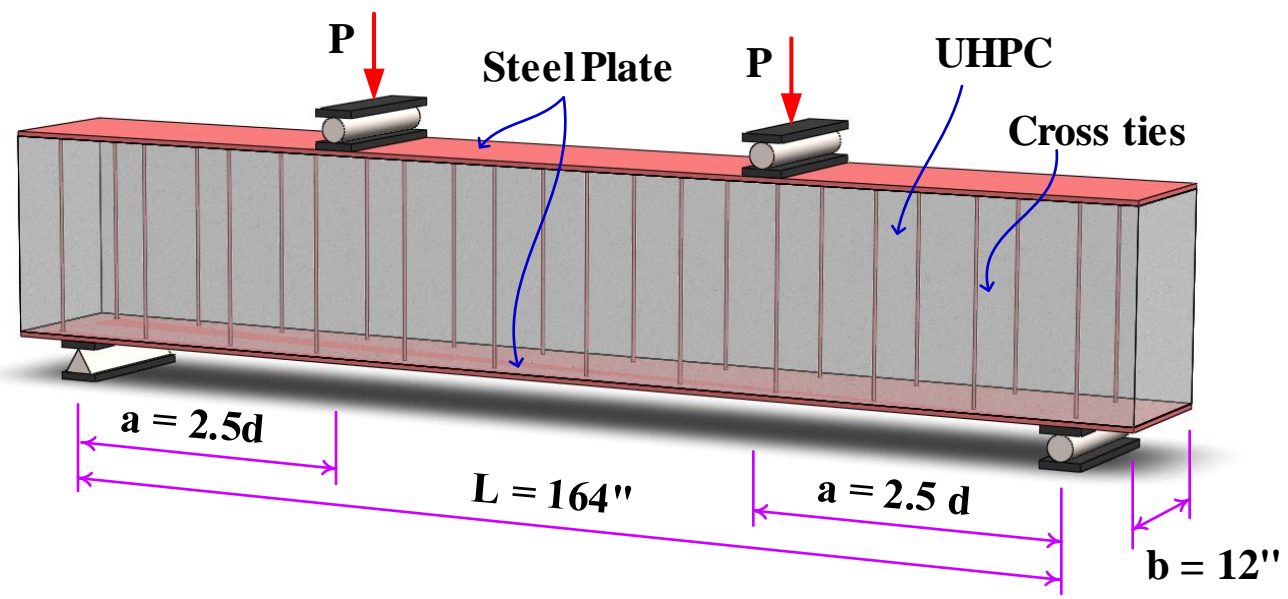
Discussion on Debonding (Continued)

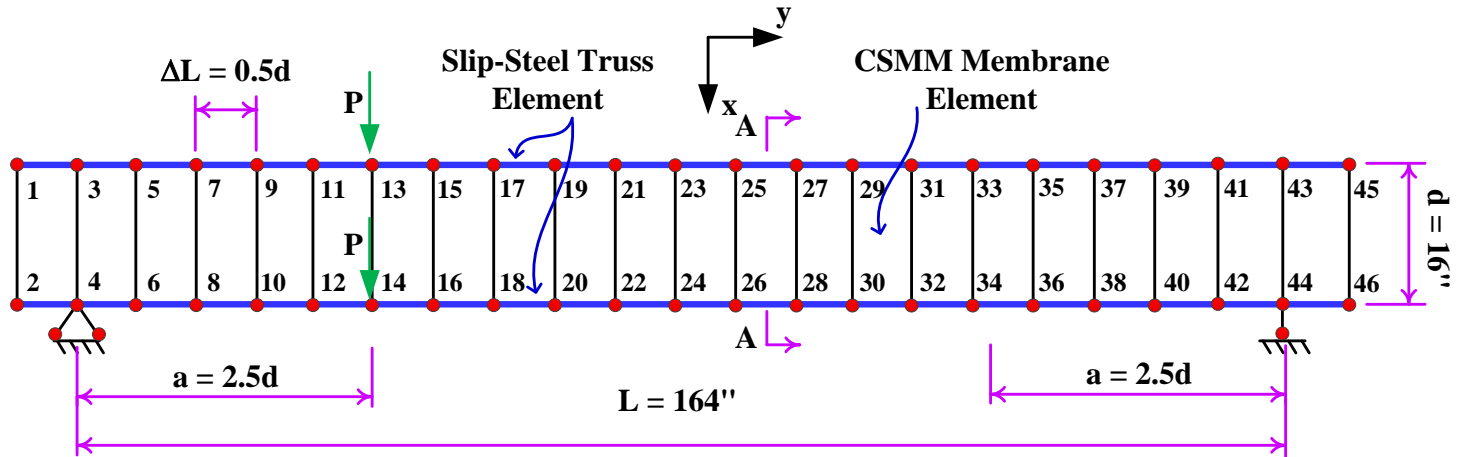
DIC images of SC3 at north-east side (a–g), showing major strain map with increasing the load.

1. DIC technique is capable of measuring concrete steel-plate bond slip and debonding.
2. Steel–plate concrete in SC beam has perfect bond until the occurrence of the first crack.

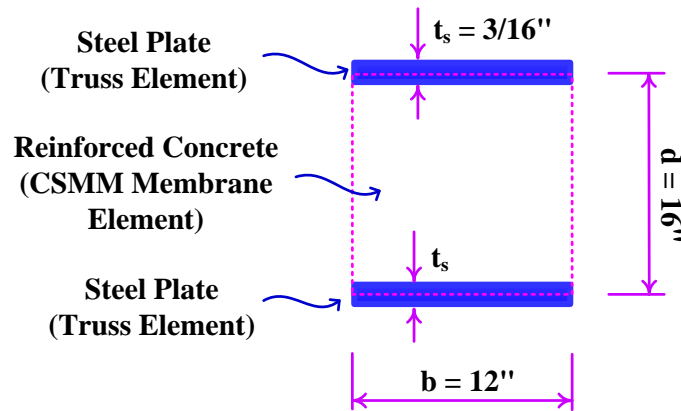


Calibrated Finite Element Model for S-UHPC Beam



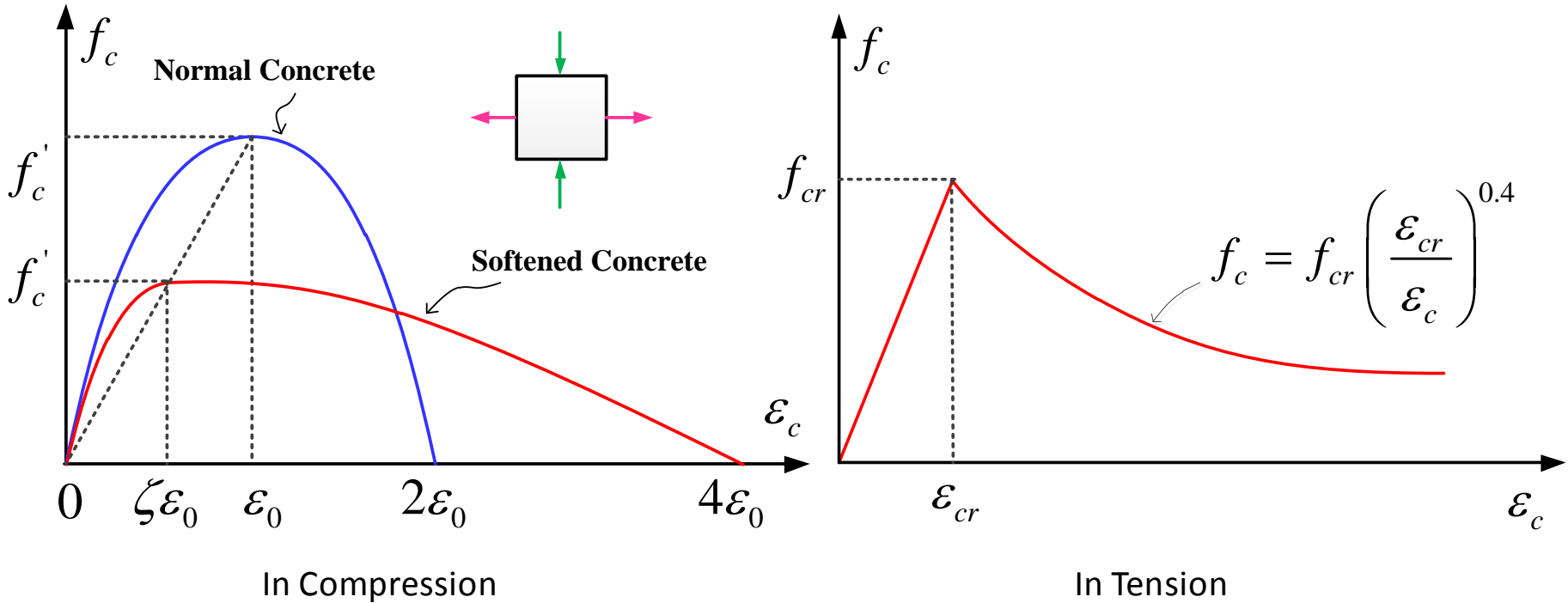


Finite Element Mesh



Cross Section A-A

Constitutive Model for Concrete



$$f_{cr} = 0.31\sqrt{f'_c \text{ (MPa)}} = \text{cracking stress}$$

$$\varepsilon_{cr} = 0.00008 = \text{cracking strain}$$

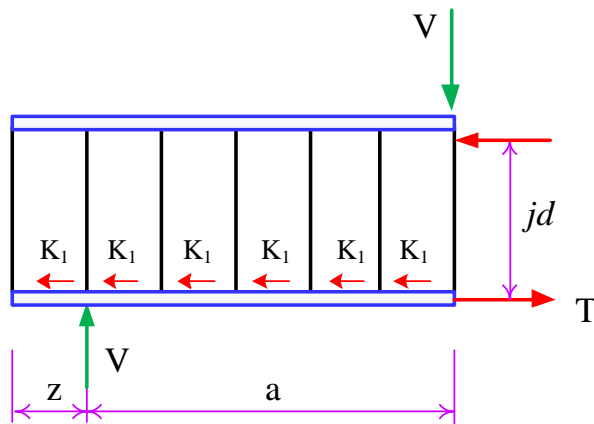
$$f'_c = \text{compressive strength}$$

$$\varepsilon_0 = \text{strain at maximum stress}$$

$$\zeta = \text{softening coefficient}$$

$$\zeta = \left(\frac{5.8}{\sqrt{f'_c \text{ (MPa)}}} \right) \left(\frac{1}{\sqrt{1+400\bar{\varepsilon}_T}} \right) \left(1 - \frac{|\beta|}{24^\circ} \right) \leq 0.9$$

Calibration of the maximum bond strength between concrete and steel plate



Free-body Diagram

Equilibrium equation:

$$V_{\max} \cdot a = jd \cdot T_{\max} \quad (\text{Eq. 1})$$

$$T_{\max} = (K_1 + 0.8\rho_v f_{yv})b(z + a) \quad (\text{Eq. 2})$$

From Eq. (1) & (2) gives:

$$K_1 = \frac{V_{\max} a}{jdb(z + a)} - 0.8\rho_{sv} f_{yv} \quad (\text{Eq. 3})$$

K_1 = the maximum bond strength between concrete and steel plate

Calibration (Continued)



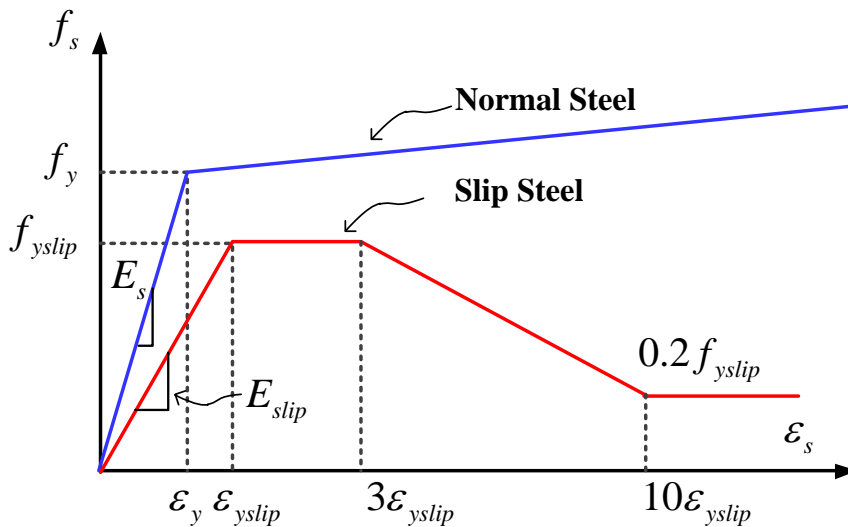
S-UHPC Beams

Specimen	b (mm)	t (mm)	a/d	ρ (%)	f_y (MPa)	f_c (Mpa)	jd (mm)	Vmax (kN)	$0.8\rho f_y$ (MPa)	T (kN)	K1 (MPa)
S-UHPC1 South	305	6.350	2.5	0.184	413	154	402	220.47	0.608	612.4	1.060
S-UHPC2 South	305	6.350	2.5	0.274	413	154	402	345.66	0.905	960.2	1.709
S-UHPC2 North	305	6.350	2.5	0.321	413	154	402	382.21	1.061	1061.7	1.830

SC Beams

Specimen	b (mm)	t (mm)	a/d	ρ (%)	f_y (MPa)	f_c (Mpa)	jd (mm)	Vmax (kN)	$0.8\rho f_y$ (MPa)	T (kN)	K1 (MPa)
SC1 North	305	4.763	2.5	0.102	413	56	402	121.71	0.337	338.1	0.584
SC1 South	305	4.763	2.5	0.102	413	56	402	116.37	0.337	323.3	0.543
SC3 North	305	4.763	2.5	0.137	413	40	402	155.35	0.453	431.5	0.722
SC3 South	305	4.763	2.5	0.137	413	40	402	143.45	0.453	398.5	0.632
SC4 North	305	4.763	2.5	0.164	413	51	402	190.04	0.542	527.9	0.896
SC4 South	305	4.763	2.5	0.205	413	51	402	235.69	0.677	654.7	1.105
SC5 South	305	4.763	1.5	0.137	413	55	402	248.77	0.453	414.6	1.241
SC5 North	305	4.763	1.5	0.164	413	55	402	287.99	0.542	480.0	1.419
SC6	305	4.763	5.2	0.137	413	55	402	127.58	0.453	737.1	0.604

Calibrated Constitutive Model for Slip Steel Plate



$$f_{yslip} = \frac{(z + a)}{t} (0.8\rho_{sv}f_{yv} + K_1)$$

$$E_{slip} = E_s \left(0.89 - 0.073 \frac{a}{d} \right)$$

f_{yslip} = yielding stress of the slip steel plate

E_{slip} = elastic modulus of the slip steel plate

K_1 = the maximum bond strength between concrete and steel plate

$$K_1 = 0.89\rho_v\sqrt{f'_c}\left(\frac{a}{d}\right)^{-0.7} \quad \text{S-UHPC Beams}$$

$$K_1 = 1.54\rho_v\sqrt{f'_c}\left(\frac{a}{d}\right)^{-0.7} \quad \text{SC Beams}$$

a = shear span of the beam

d = depth of the beam

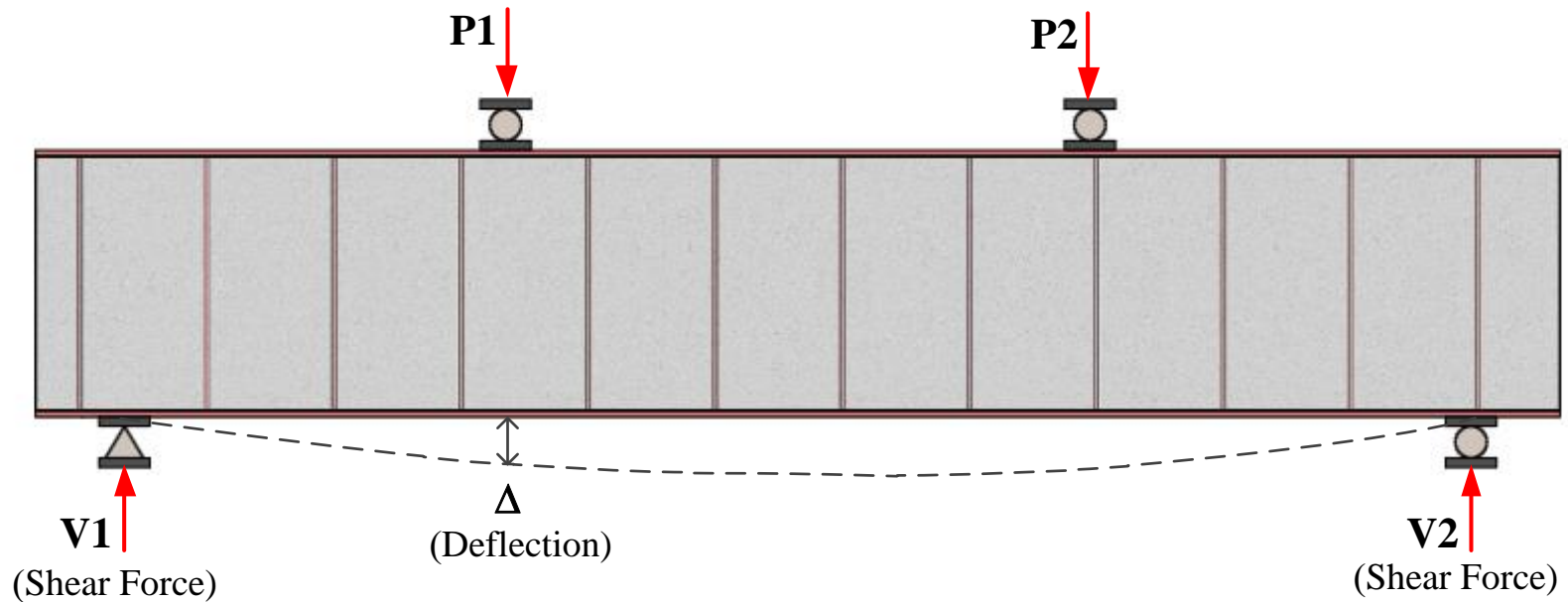
z = distance from center of support to the end beam

ρ_{sv} = percentage of transverse steel bar

f_{yv} = yielding stress of transverse steel bar

λ = deterioration rate

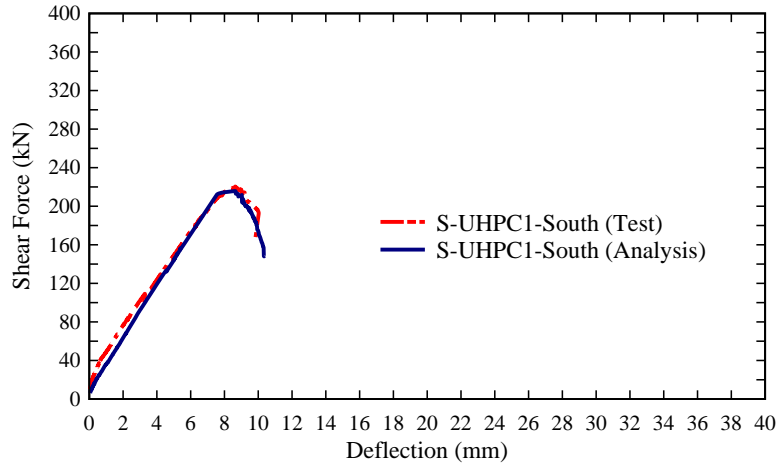
Comparison of Analytical Results with Experimental Outcomes



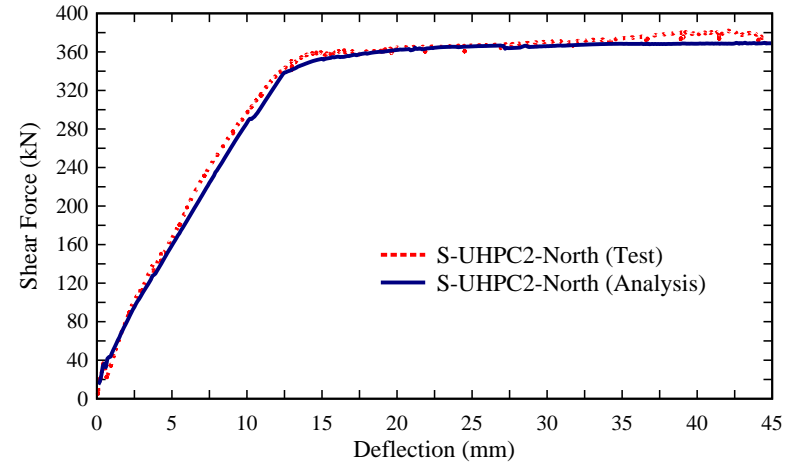


Comparison (Continued)

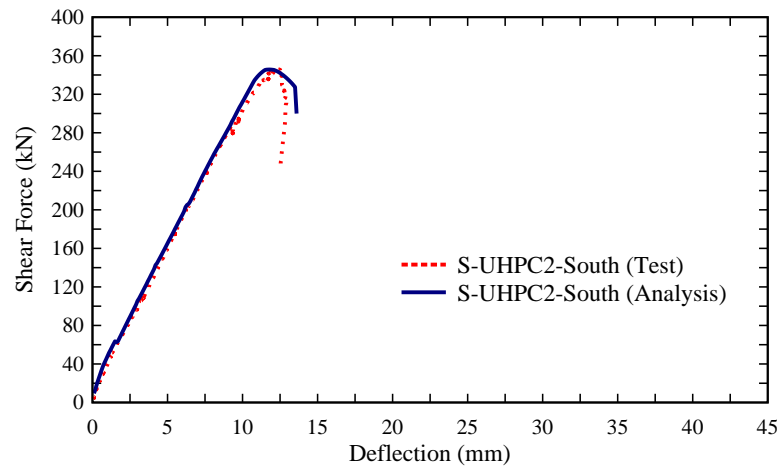
S-UHPC-1 (South)



S-UHPC-2 (North)



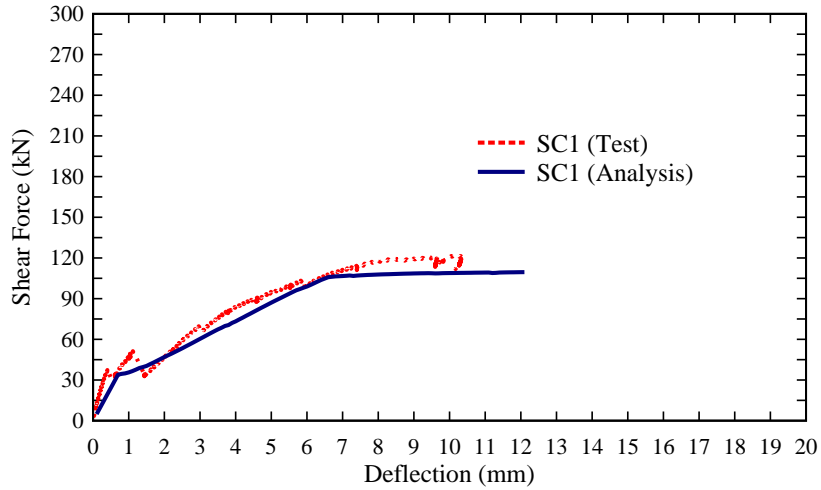
S-UHPC-2 (South)



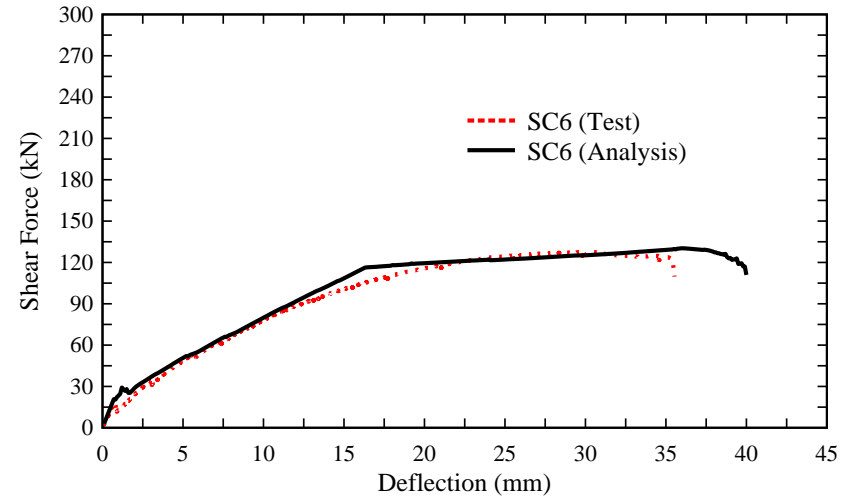


Comparison (Continued)

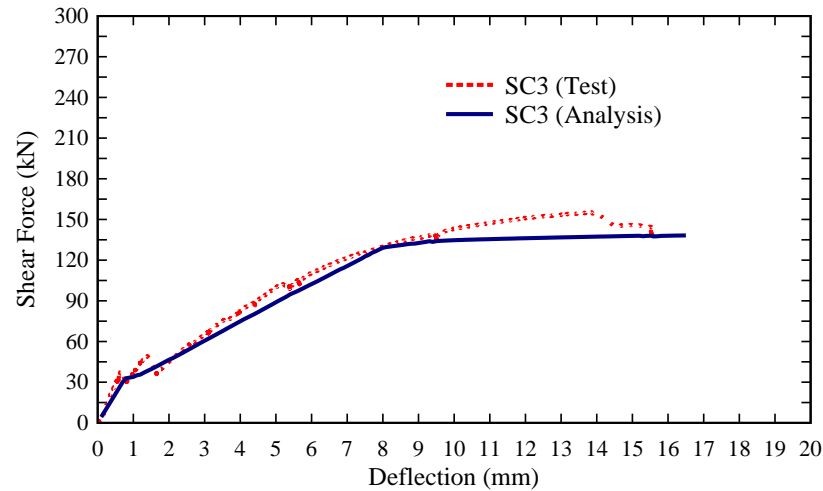
Beam SC1



Beam SC6

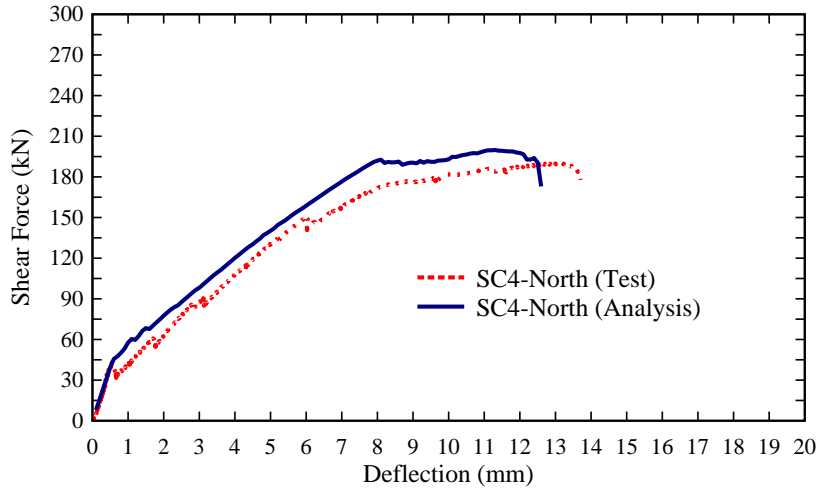


Beam SC3

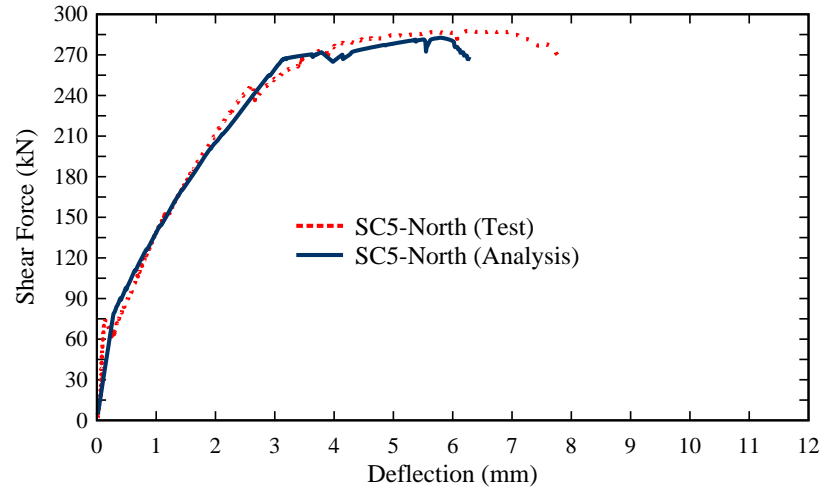


Comparison (Continued)

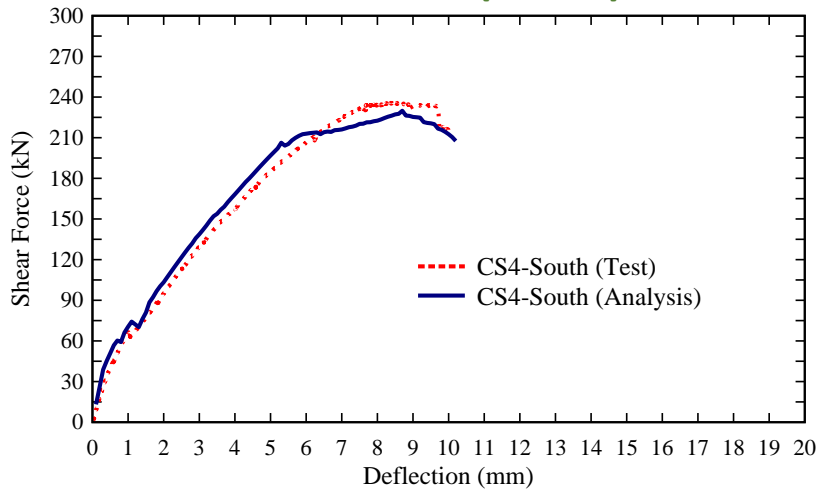
Beam SC4 (North)



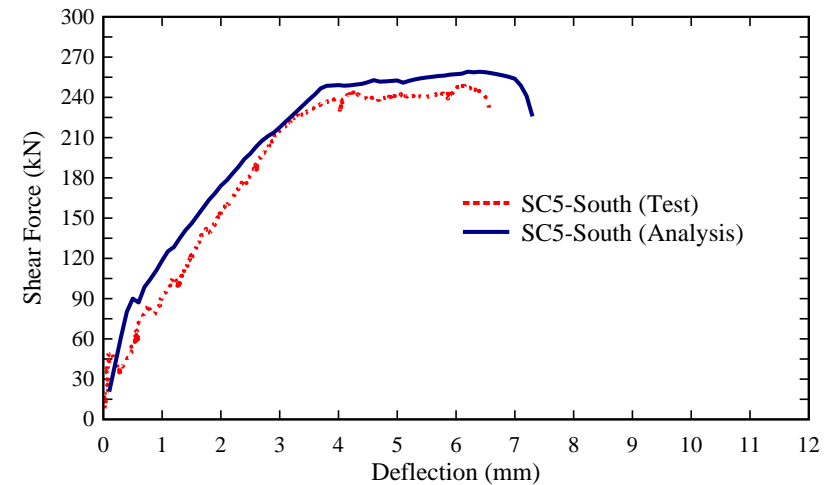
Beam SC5 (North)



Beam SC4 (South)



Beam SC5 (South)



Conclusions

- The developed UHPC material can be robustly processed at **large scale** with commercially available ingredients and equipment.
- It meets **self-consolidating** and **compressive strength** requirements.
- **Particle size distribution** for optimum packing density, the **physical and chemical parameters** of ingredients, and the resulting **microstructure** after hydration are considered essential for the design of self-consolidating UHPC.
- **Brittle** failure if **insufficient cross ties** are provided. Results show that cross ties can effectively improve interfacial bond condition, ductility and shear strength of SC and S-UHPC beams.

Conclusions

- For S-UHPC Beams: 10% more than that specified in ACI code when $a/d=2.5$.

- For SC Beams:

$$\rho_{t,min} = 1.45 \times \rho_{t,ACI} \quad \text{for } 2.0 < a/d < 4.0, \text{ or}$$

$$\rho_{t,min} = 1.25 \times \rho_{t,ACI} \quad \text{for } a/d \leq 2.0 \text{ and } a/d \geq 4.0.$$

- DIC technique is capable of measuring concrete steel-plate bond slip and debonding.
- PZT smart aggregates provide early warning about the debonding of the steel plate and the concrete in SC beams before structural failure happens.
- The bond slip based stress-strain curve of steel plate is developed that can be used to accurately predict the shear force deflection relationship of SC beams.



Thank you.